

IN-34
388486

TECHNICAL NOTE

D-893

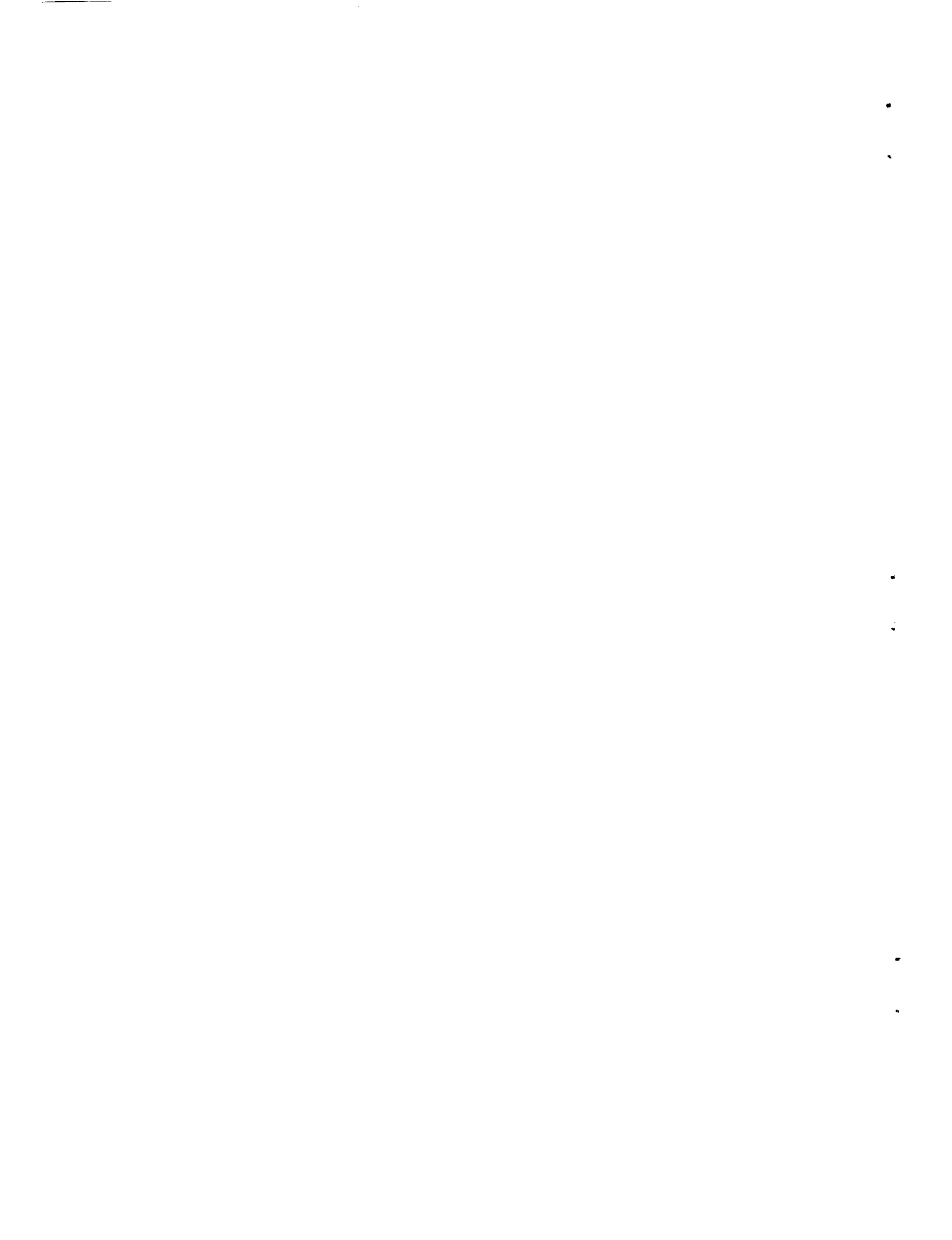
PRESSURE LOADS PRODUCED ON A FLAT-PLATE WING BY ROCKET
JETS EXHAUSTING IN A SPANWISE DIRECTION BELOW THE
WING AND PERPENDICULAR TO A FREE-STREAM
FLOW OF MACH NUMBER 2.0

By Ralph A. Falanga and Joseph J. Janos

Langley Research Center
Langley Field, Va.

NATIONAL AERONAUTICS AND SPACE ADMINISTRATION
WASHINGTON

May 1961



TECHNICAL NOTE D-893

PRESSURE LOADS PRODUCED ON A FLAT-PLATE WING BY ROCKET

JETS EXHAUSTING IN A SPANWISE DIRECTION BELOW THE
WING AND PERPENDICULAR TO A FREE-STREAM

FLOW OF MACH NUMBER 2.0¹

L
1
6
1
4

By Ralph A. Falanga and Joseph J. Janos

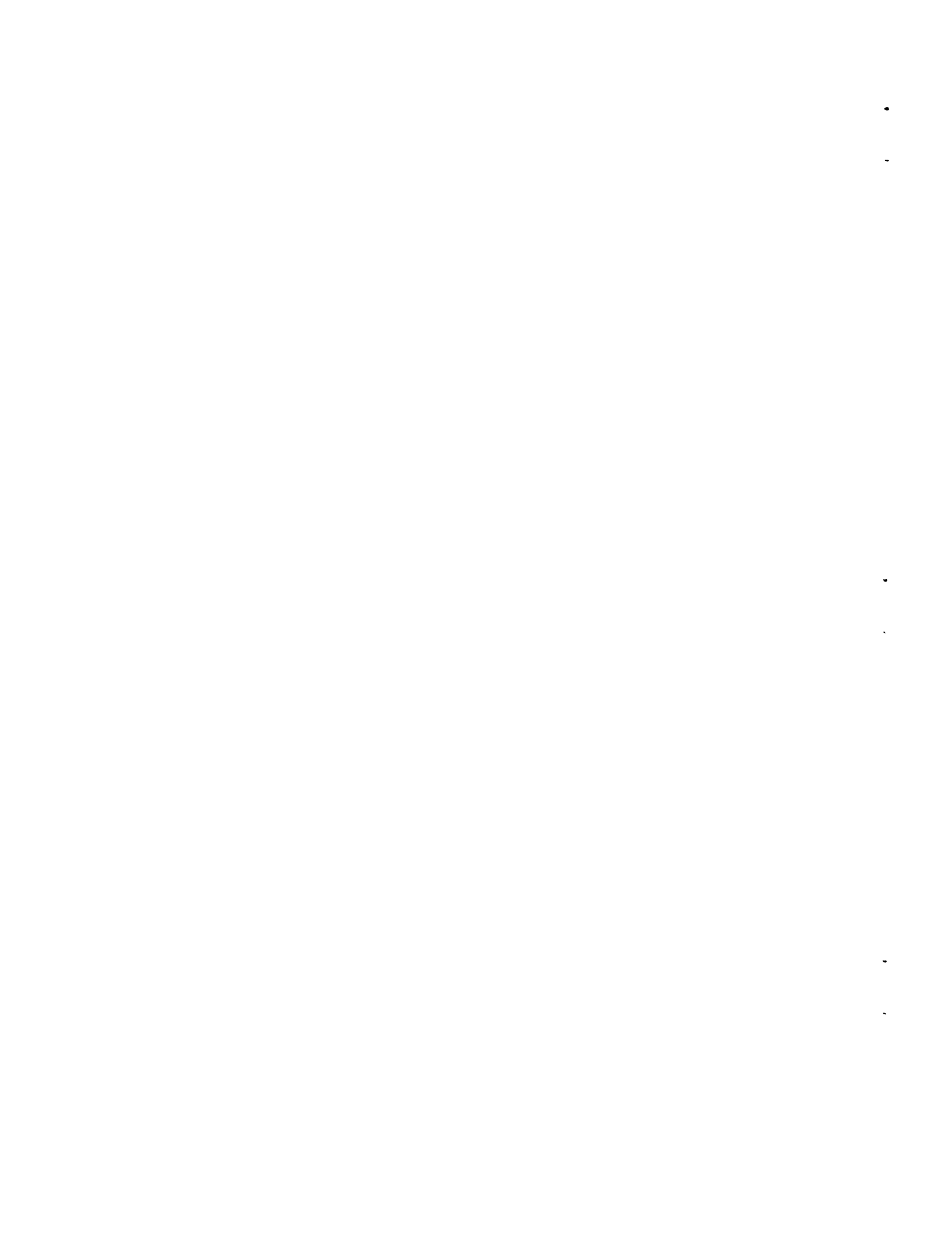
SUMMARY

An investigation at a Reynolds number per foot of 14.4×10^6 was made to determine the pressure loads produced on a flat-plate wing by rocket jets exhausting in a spanwise direction beneath the wing and perpendicular to a free-stream flow of Mach number 2.0. The ranges of the variables involved were (1) nozzle types - one sonic (jet Mach number of 1.00), two supersonic (jet Mach numbers of 1.74 and 3.04), and one two-dimensional supersonic (jet Mach number of 1.71); (2) vertical nozzle positions beneath the wing of 4, 8, and 12 nozzle-throat diameters; and (3) ratios of rocket-chamber total pressure to free-stream static pressure from 0 to 130.

The incremental normal force due to jet interference on the wing varied from one to two times the rocket thrust and generally decreased as the pressure ratio increased. The chordwise coordinate of the incremental-normal-force center of pressure remained upstream of the nozzle center line for the nozzle positions and pressure ratios of the investigation. The chordwise coordinate approached zero as the jet vertical distance beneath the wing increased. In the spanwise direction there was little change due to varying rocket-jet position and pressure ratio. Some boundary-layer flow separation on the wing was observed for the rocket jets close to the wing and at the higher pressure ratios. The magnitude of the chordwise and spanwise pressure distributions due to jet interference was greatest for rocket jets close to the wing and decreased as the jet was displaced farther from the wing.

The design procedure for the rockets used is given in the appendix.

¹Supersedes NACA Research Memorandum L58D09 by Ralph A. Falanga and Joseph J. Janos, 1958.





APPARATUS

Preflight Jet Facility

The tests were conducted in the preflight-jet facility of the Langley Pilotless Aircraft Research Station at Wallops Island, Va. A description of this facility is given in reference 2. A Mach number 2.0, 27-inch-square nozzle was used for all tests. A photograph of the test setup is shown as figure 1.

Wing

A steel flat plate, 1/2 inch thick, was used to simulate a two-dimensional wing and this plate was made to span the exit (27-inch) nozzle. The wing was welded to supports that were bolted to the exit flange of the preflight-jet nozzle. The leading edge of the wing had an 8° bevel on the upper surface and protruded approximately 3 inches upstream into the preflight-jet nozzle exit. The wing had a rectangular plan form and a chord of $16\frac{3}{8}$ inches. Static-pressure orifices were installed on the wing lower surface and their positions are shown in figure 2.

Vertical Strut

The vertical plate which was bolted to the wing was fabricated from 1/2-inch-thick steel plate. The leading edge was beveled to 18° and was located 1.5 inches upstream of the exit plane of the preflight-jet nozzle exit. The strut was located 3 inches from the side wall of the jet. This was done to keep the strut free of the boundary-layer buildup present along the tunnel nozzle wall. The strut had a chord of 15 inches and included provisions for mounting rocket motors in three positions: A, B, and C. These positions were located at x/D_T of 24, 17.5, and 10.5 downstream of the strut and z/D_T of 4, 8, and 12 beneath the flat-plate wing. The rocket-nozzle exits were faired with the inner surface of the vertical strut, and located downstream of these nozzle exits were a total of nine static-pressure orifices. Figure 2 illustrates the arrangement of the flat-plate wing, vertical strut, and rocket-nozzle locations. This figure also shows the locations of the strut orifices.

Rockets

Figure 3 is a detailed drawing of the rocket nozzles used in the investigation. The throat areas were the same for all the rocket

nozzles; thus, the two-dimensional nozzle has an equivalent throat diameter equal to the throat diameter of the axisymmetric nozzles. The rectangular exit of the two-dimensional nozzle was oriented such that the long side of the rectangular section was vertical. All distances from nozzle exits are expressed in terms of nozzle-throat diameters or equivalent throat diameter.

Specially designed solid-propellant rockets generated the hot exhaust gases ($\gamma = 1.25$). These rockets were designed to give a triangular chamber-pressure impulse and to operate within a range of 0 to 1,800 pounds per square inch in a time interval of 0.8 second. (See fig. 4.) The range of chamber pressure varied some from rocket to rocket because of variations in burning characteristics of the solid propellants and, also, because of different amounts of nozzle losses. A detailed description of the design, performance, and components of the rockets is given in the appendix.

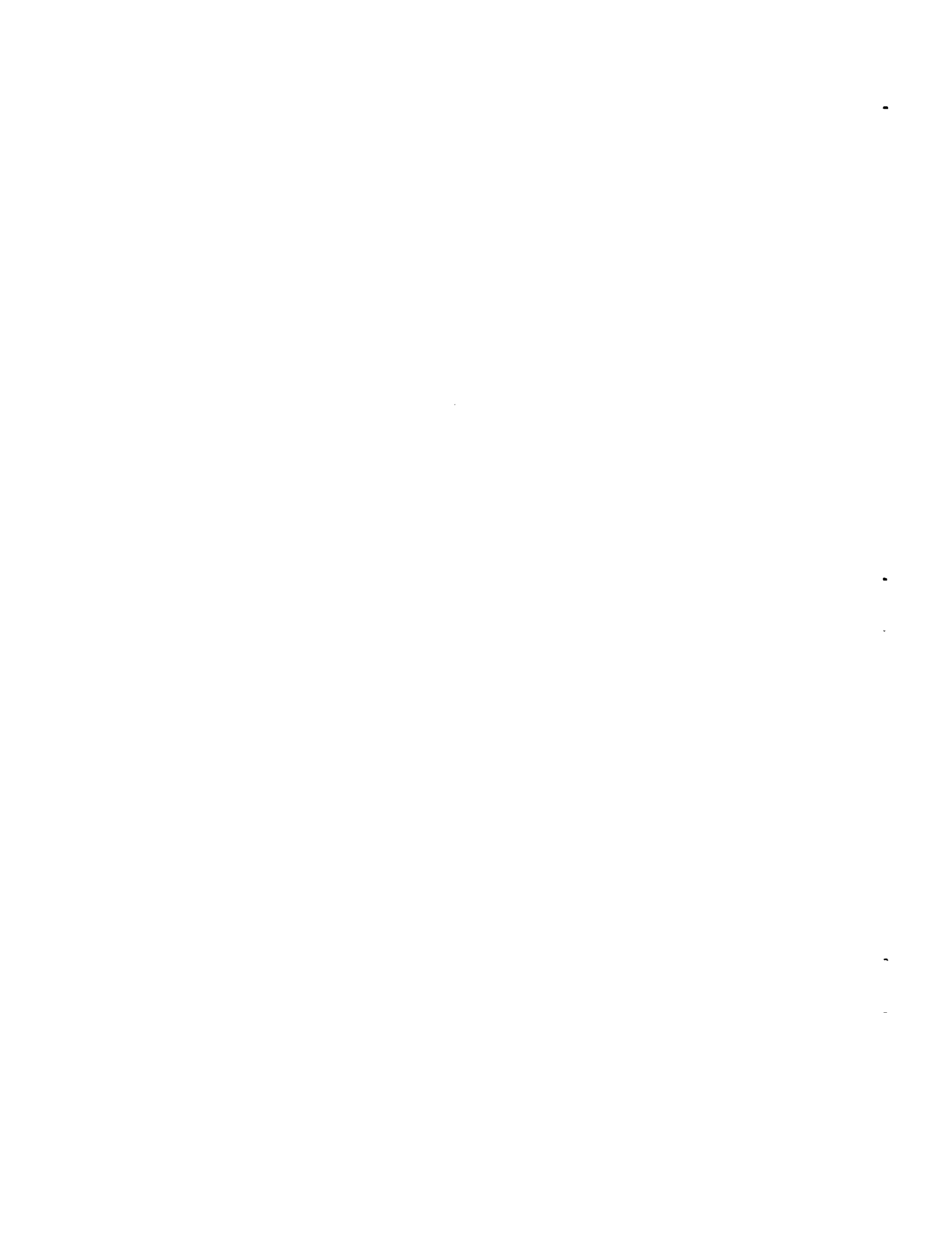
INSTRUMENTATION

The pressures at the head end of the rocket chamber were measured for all tests. The pressure distributions on the flat-plate wing were measured by Statham pressure gages and by two 6-cell pressure units. These gages and cells were connected to 0.06-inch-diameter wing orifices by 1/8-inch copper tubing. The chordwise and spanwise locations of these wing static-pressure orifices are shown in figure 2.

Nine static-pressure orifices 0.06 inch in diameter supplied some static-pressure data on the inner surface of the vertical strut. The locations for these orifices are also shown in figure 2. The free-stream total and static pressures of the preflight-jet nozzle exit were measured for all tests so that free-stream dynamic pressure and pressure coefficients could be computed. Four oscillograph recorders and two 6-cell pressure recorders were used to register all the data obtained for this investigation.

ACCURACY

The accuracy of the measurements, based on instrument accuracy and errors in reading and plotting the data, was estimated to vary within the following limits:



T-1614

the jet exit to oblique in the spanwise direction. This shock pattern exhibits the same characteristics in the vertical plane. The region between the primary shock wave and jet boundary will experience positive pressures and the magnitude of these positive pressures will diminish as the primary shock-wave angle decreases with respect to the stream direction. The pressure reaches a positive peak at the primary shock and then an expansion of the flow causes negative pressures. Then, a recompression brings the negative values to slightly below free-stream conditions. This recompression may be due to a wake shock (considering the jet as a solid body), a jet shock originating within the jet, or a combination of both. Schlieren photographs of some actual flow fields existing about side jets exhausting into supersonic main streams are shown in reference 1.

RESULTS AND DISCUSSION

Wing pressure data are presented in tables 1 to 10 as incremental pressure coefficients for the following variables: nozzle geometry, nozzle position, and pressure ratio. The effects of these variables on wing pressure distributions (as a result of shock location and boundary-layer separation), loads, and centers of pressure are discussed in the following sections. Because of insufficient pressure data on the strut, no discussion of the incremental vertical-strut pressures is made; only the tabulated data (tables 11 to 14) are presented.

Incremental Wing Pressures

Since the rocket-chamber pressures varied during each test, values of ΔC_p for $p_{t,c}/p_\infty$ in increments of 10 have been given in tables 1 to 10. The variations of chordwise and spanwise ΔC_p are presented for a value of $p_{t,c}/p_\infty$ of 58 in figures 6 to 9 and for a value of $p_{t,c}/p_\infty$ of 120 in figure 10. In general, these plots show the same characteristics: namely, in the chordwise direction the pressure rises to maximum values, then a rapid expansion of the flow causes negative coefficients, and a recompression brings the negative values to near free-stream conditions. In the spanwise direction ΔC_p diminishes in magnitude from a maximum near the nozzle exit to near free-stream conditions at distances greater than 30 nozzle throat diameters from the exit.

These plots also indicate that the effects on pressure distributions due to nozzle geometries were small; whereas, the effects on induced wing pressures due to nozzle position and pressure ratio appear to be more pronounced. The induced pressures were the greatest when the rocket jets were located at position A and were the least at position C. As the pressure ratio was increased, the magnitude of the

induced wing pressures also increased. These results were due mainly to the angle the primary shock makes with the wing at the intersection point. For the rocket jets close to the wing (position A), the angle was the greatest and, hence, the magnitude of the induced pressures was the greatest. Increasing the pressure ratio increased the shock angle and thus caused even greater induced pressures on the wing. (See figs. 7 and 10 for a comparison of pressure distributions for nozzle position A at values of $p_{t,c}/p_\infty$ of 58 and 120.)

The fact that the more intense portion of the primary shock intersected the wing for positions A and B rather than for position C for all nozzle types caused the boundary-layer flow to separate in some regions forward of the primary shock for positions A and B. This is evident from the initial shape of the chordwise pressure-distribution curves, as reported in references 3 and 4 for turbulent separated flow, since the initial portions of the pressure-distribution curves have a double peak. The chordwise pressure variations (up to the maximum peak point) obtained at y/D_T of 2.5 for the sonic nozzle in positions A and B were similar to that observed about a forward-facing step with separated boundary layer in reference 3. An incremental pressure coefficient of approximately 0.35 measured for the first pressure peaks from distributions for positions A and B agreed favorably with the turbulent-boundary-layer value (0.335) measured on a flat plate from the step technique of reference 3 at a free-stream Mach number of 2.0.

Integrated Loads

The incremental force obtained was divided by the rocket thrust and this force ratio is plotted as a function of pressure ratio in figure 11. The force ratio varied approximately between 1 and 2 and generally decreased with increasing pressure ratio. Figure 11(a) shows that, generally, at any pressure ratio the force ratio decreases as the sonic nozzle is moved away from the wing. This is the same result that was obtained in reference 6 for jets exhausting downstream. Figure 11(b) shows that the two-dimensional supersonic nozzle ($M_j = 1.71$) induced loads that were about half as large as those induced by the $M_j = 1.0$ and 1.74 nozzles; whereas, the $M_j = 3.04$ nozzle induced loads that were about 70 percent as large.

Center of Pressure

The variation of incremental normal-force center of pressure for chordwise and spanwise directions is illustrated in figure 12 for only one case, that of the sonic nozzle operating at $p_{t,c}/p_\infty$ of 50, 75, and 100.

APPENDIX

DESIGN PROCEDURE FOR ROCKETS EMPLOYED

In order to illustrate the design procedure, the actual rocket parameters which were required for this investigation are used herein and are presented as follows:

Range of $P_{t,c}/P_\infty$ from 0 to 130

Relative symmetric time-history variation of $P_{t,c}/P_\infty$

Rocket operating time of 0.6 to 0.8 second

Back pressure P_∞ of 14.7 pounds per square inch absolute

Internal Ballistics Relationships

For the rocket operating at equilibrium conditions, the mass rate of gases generated by combustion of the solid propellant must be equal to the mass rate of gases discharged through the rocket nozzle - namely,

$$m_g = m_d \quad (1)$$

The mass rate of gases generated is a function of the solid-propellant density, the exposed propellant area, and the linear burning rate of the propellant, which can be written as

$$m_g = \rho S b \quad (2)$$

where the linear burning rate is defined as

$$b = C P_{t,c}^n \quad (3)$$

Substituting equation (3) into equation (2) gives

$$m_g = \rho S C P_{t,c}^n \quad (4)$$

where

- C coefficient in equation (3) which is a function of propellant
 $p_{t,c}$ rocket-chamber total pressure, lb/sq in.
 n function of propellant
 ρ density of solid propellant, lb/cu in.
 S exposed solid-propellant area to combustion flame, sq in.

L1614
 From equation (1), the mass rate of gases discharged can be written as a function of a discharge coefficient, rocket nozzle-throat area, and rocket-chamber total pressure:

$$m_d = C_D A_t p_{t,c} \quad (5)$$

where C_D , the discharge coefficient, is defined as the mass rate of flow possible when a given powder composition is burned in a rocket motor having a unit throat area and a unit chamber pressure. The discharge coefficient C_D remains relatively constant throughout the combustion process. Thus, the burning surface of the solid propellant must vary according to the following equations:

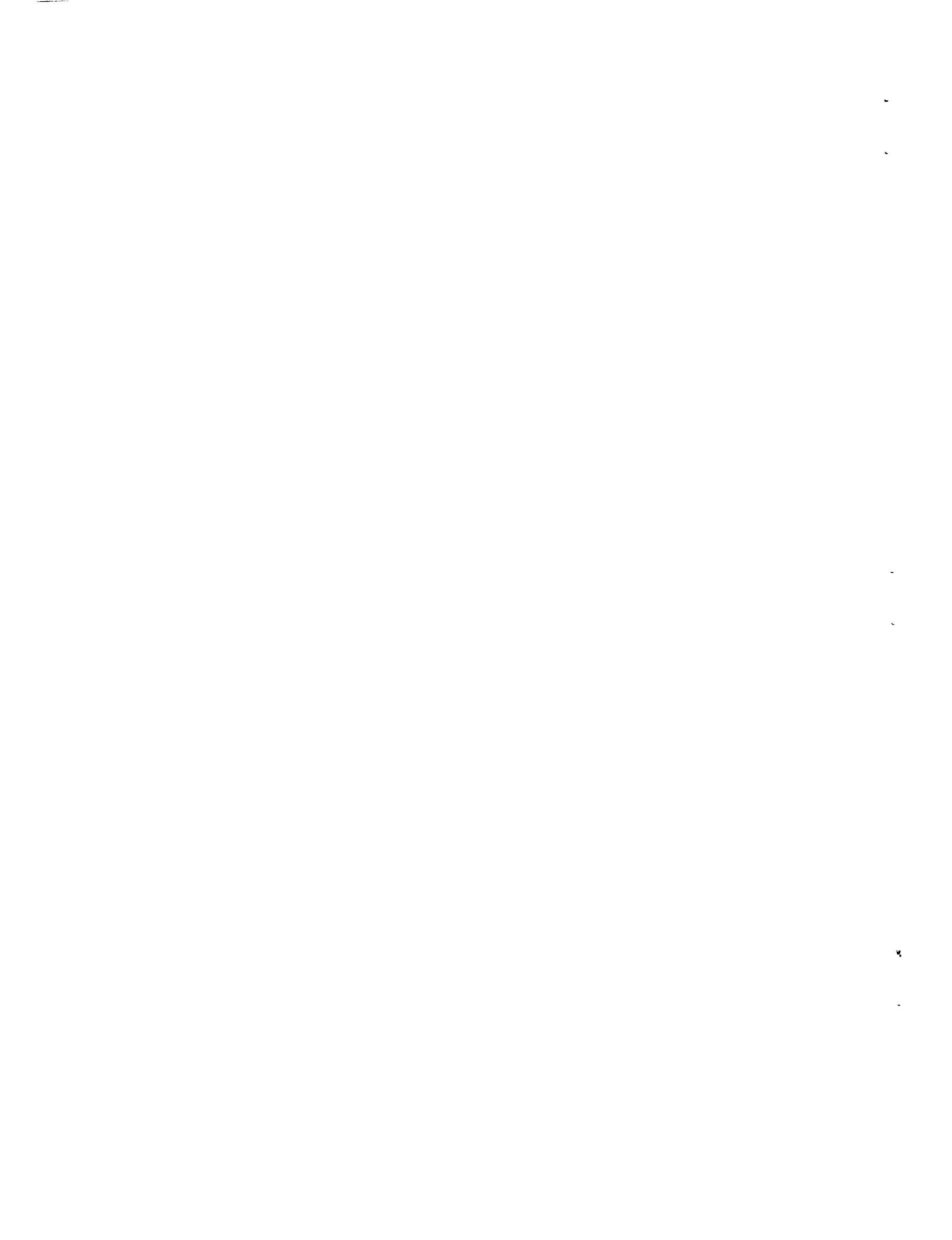
$$S = \frac{C_D A_t p_{t,c}}{\rho b} \quad (6a)$$

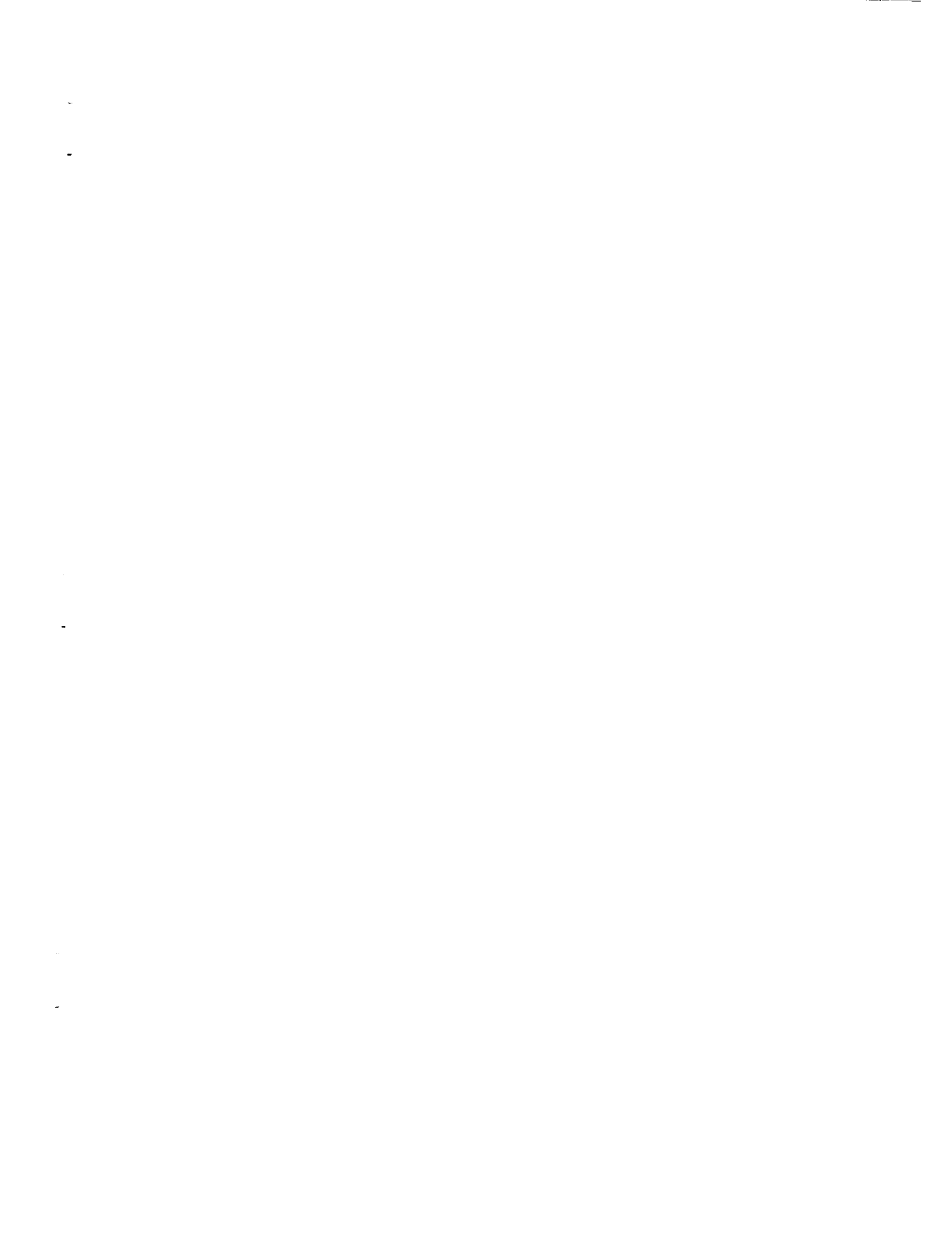
or

$$S = \frac{C_D A_t}{\rho C} (p_{t,c})^{1-n} \quad (6b)$$

Propellant Design

In order to cover the desired pressure-ratio range for this investigation, the combustion-chamber pressure was varied as shown in the following diagram:





values, and for comparison the actual results for two of the firings have been superposed upon the design curve which is shown in figure 15.

Calibration Curves

The rocket thrust and chamber pressure were measured during each static firing, and calibration curves of rocket-chamber pressure as a function of jet-exit static pressure for each nozzle type has been obtained. These curves are shown in figure 16. The jet-exit static pressure was obtained from the thrust equation:

$$F_J = p_J A_J (\gamma M_J^2 + 1) - p_\infty A_J \quad (7)$$

by solving for p_J

$$p_J = \frac{F_J + p_\infty A_J}{A_J (\gamma M_J^2 + 1)} \quad (8)$$

where

A_J jet-exit area, sq in.

γ ratio of specific heats for the propellant ($\gamma = 1.25$)

M_J Mach number at jet exit

p_∞ free-stream static pressure, lb/sq in. abs

p_J jet-exit static pressure, lb/sq in. abs

Since the rocket-chamber pressures were measured during each tunnel run, the thrust of the rockets was obtained by choosing values of p_J from the calibration curves and computing by use of equation (7) the thrust for the existing back pressure.

REFERENCES

1. Morkovin, M. V., Pierce, C. A., Jr., and Craven, C. E.: Interaction of a Side Jet With a Supersonic Main Stream. Bull. No. 35, Eng. Res. Inst., Univ. of Michigan, Sept. 1952.
2. Faget, Maxime A., Watson, Raymond S., and Bartlett, Walter A., Jr.: Free-Jet Tests of a 6.5-Inch-Diameter Ram-Jet Engine at Mach Numbers of 1.81 and 2.00. NACA RM L50L06, 1951.
3. Lange, Roy H.: Present Status of Information Relative to the Prediction of Shock-Induced Boundary-Layer Separation. NACA TN 3065, 1954.
4. Chapman, Dean R., Kuehn, Donald M., and Larson, Howard K.: Preliminary Report on a Study of Separated Flows in Supersonic and Subsonic Streams. NACA RM A55L14, 1956.
5. Braslow, Albert L.: Effect of Distributed Granular-Type Roughness on Boundary-Layer Transition at Supersonic Speeds With and Without Surface Cooling. NACA RM L58A17, 1958.
6. Leiss, Abraham, and Bressette, Walter E.: Pressure Distribution Induced on a Flat Plate by a Supersonic and Sonic Jet Exhaust at a Free-Stream Mach Number of 1.80. NACA RM L56I06, 1957.

TABLE 1.- WING PRESSURES FOR SONIC NOZZLE AT POSITION A

TABLE 2.- WING PRESSURES FOR SONIC NOZZLE AT POSITION B

Orifice ordinates		Incremental wing pressure coefficients for $p_{t,c}/p_\infty$ of -												
x/D _T	y/D _T	10	20	30	40	50	60	70	80	90	100	110	120	130
11.5	2.5			0.001	0.004	0.006	0.006	0.009	0.016	0.030	0.054			
14.0	2.5			0	0	0	.035	.062	.082	.091	.091			
19.0	2.5			.210	.276	.422	.428	.375	.365	.373	.390			
21.5	2.5			.250	.296	.301	.312	.322	.330	.332	.340			
24.0	2.5			.148	.170	.168	.168	.168	.167	.167	.168			
26.5	2.5			.037	.045	.045	.044	.038	.035	.030	.028			
29.0	2.5			.041	-.049	-.056	-.061	-.064	-.068	-.072	-.077			
34.0	2.5			-.066	-.096	-.115	-.127	-.136	-.142	-.146	-.147			
39.0	2.5			-.016	-.030	-.040	-.045	-.060	-.070	-.074	-.075			
44.0	2.5			-.011	-.017	-.019	-.016	-.016	-.021	-.035	-.037			
49.0	2.5			----	----	----	----	----	----	----	----			
54.0	2.5			-.009	-.010	-.013	-.014	-.015	-.015	-.016	-.016			
64.0	2.5			-.005	-.007	-.011	-.013	-.014	-.014	-.015	-.015			
11.5	7.5			0	0	0	0	0	0	0	0			
14.0	7.5			0	0	0	0	.020	.055	.091	.143			
19.0	7.5			.102	.175	.229	.268	.301	.331	.356	.374			
21.5	7.5			.198	.248	.271	.283	.300	.318	.335	.353			
24.0	7.5			.185	.195	.205	.212	.227	.240	.246	.254			
26.5	7.5			.042	.045	.045	.046	.047	.048	.047	.045			
31.5	7.5			-.030	-.038	-.045	-.050	-.057	-.062	-.070	-.075			
36.5	7.5			-.050	-.070	-.092	-.100	-.104	-.108	-.115	-.117			
41.5	7.5			-.025	-.042	-.065	-.075	-.090	-.100	-.111	-.115			
46.5	7.5			-.015	-.016	-.014	-.012	-.015	-.017	-.022	-.029			
51.5	7.5			-.006	-.008	-.009	-.011	-.012	-.012	-.012	-.012			
61.5	7.5			-.007	-.010	-.011	-.012	-.013	-.014	-.015	-.016			
9.0	12.5			0	0	0	0	0	0	0	0			
16.5	12.5			0	0	0	0	.010	.045	.094	.141			
19.0	12.5			0	0	.037	.095	.160	.196	.220	.235			
21.5	12.5			.035	.108	.169	.200	.230	.250	.266	.275			
24.0	12.5			.137	.192	.217	.232	.247	.258	.272	.281			
26.5	12.5			.154	.179	.185	.194	.195	.200	.204	.209			
29.0	12.5			.100	.115	.115	.115	.115	.111	.110	.110			
34.0	12.5			0	0	-.011	-.017	-.023	-.028	-.031	-.036			
39.0	12.5			-.050	-.057	-.065	-.072	-.079	-.083	-.089	-.095			
49.0	12.5			-.018	-.025	-.031	-.040	-.050	-.062	-.075	-.085			
59.0	12.5			-.007	-.009	-.010	-.011	-.010	-.012	-.010	-.007			
19.0	17.5			0	0	0	0	.021	.050	.081	.085			
24.0	17.5			.005	.039	.088	.117	.138	.150	.157	.165			
26.5	17.5			.055	.113	.145	.158	.165	.177	.183	.190			
31.5	17.5			.110	.122	.125	.126	.128	.132	.133	.135			
36.5	17.5			.056	.059	.052	.050	.046	.042	.040	.040			
41.5	17.5			-.012	-.019	-.024	-.029	-.031	-.036	-.037	-.036			
61.5	17.5			-.006	-.009	-.010	-.010	-.010	-.010	-.010	-.010			
31.5	25.0													
39.0	25.0			.083	.090	.090	.090	.090	.090	.092	.095			
54.0	25.0			-.015	-.018	-.020	-.022	-.023	-.025	-.026	-.027			
59.0	25.0			-.036	-.043	-.045	-.049	-.050	-.050	-.051	-.052			
64.0	25.0													
41.5	30.0													
46.5	30.0			.065	.065	.065	.065	.066	.067	.067	.065			
51.5	30.0													
61.5	30.0			-.015	-.016	-.017	-.018	-.019	-.020	-.020	-.020			

TABLE 3.- WING PRESSURES FOR SONIC NOZZLE AT POSITION C

Orifice ordinates		Incremental wing pressure coefficients for $p_{t,c}/p_\infty$ of -												
x/D_T	y/D_T	10	20	30	40	50	60	70	80	90	100	110	120	130
11.5	2.5	0	0	0	0	0.005	0.023	0.062	0.115	0.170				
14.0	2.5	.005	.010	.016	.022	.058	.133	.211	.275	.327	.358			
19.0	2.5	.056	.128	.203	.243	.275	.287	.297	.295	.292	.275			
21.5	2.5	.103	.148	.171	.180	.180	.180	.175	.170	.162	.150			
24.0	2.5	.078	.092	.095	.095	.095	.094	.091	.087	.086	.084			
26.5	2.5	.031	.033	.031	.030	.029	.027	.025	.023	.021	.018			
29.0	2.5	-.005	-.010	-.020	-.021	-.021	-.025	-.026	-.030	-.030	-.032			
34.0	2.5	-.037	-.055	-.077	-.087	-.095	-.100	-.105	-.108	-.110	-.112			
39.0	2.5	-.020	-.028	-.033	-.033	-.031	-.032	-.033	-.037	-.037	-.030			
44.0	2.5	-.011	-.017	-.021	-.024	-.025	-.032	-.045	-.050	-.046	-.043			
49.0	2.5	-.010	-.013	-.014	-.015	-.016	-.020	-.022	-.025	-.022	-.020			
54.0	2.5	0	0	-.005	-.005	-.005	-.007	-.007	-.010	-.010	-.012			
64.0	2.5	0	0	0	0	0	0	0	0	0	0			
11.5	7.5	0	.003	.005	.005	.005	.005	.005	.006	.019	.056			
14.0	7.5	0	0	.002	.005	.005	.027	.110	.187	.242	.272			
19.0	7.5	.038	.110	.184	.238	.268	.285	.295	.305	.311	.315			
21.5	7.5	.069	.162	.193	.205	.210	.215	.217	.217	.218	.220			
24.0	7.5	.110	.132	.130	.128	.128	.125	.124	.123	.122	.122			
26.5	7.5	.020	.025	.026	.025	.024	.022	.020	.019	.016	.016			
31.5	7.5	-.025	-.030	-.035	-.036	-.038	-.044	-.046	-.053	-.058	-.064			
36.5	7.5	-.040	-.060	-.070	-.080	-.087	-.092	-.096	-.100	-.103	-.102			
41.5	7.5	-.016	-.021	-.021	-.023	-.026	-.030	-.043	-.070	-.090	-.100			
46.5	7.5	-.015	-.024	-.028	-.028	-.025	-.027	-.040	-.045	-.045	-.035			
51.5	7.5	-.010	-.014	-.012	-.009	-.011	-.012	-.015	-.014	-.013	-.012			
61.5	7.5	0	0	0	0	0	0	0	0	0	0			
9.0	12.5	0	0	0	0	0	0	0	0	0	0			
16.5	12.5	0	0	0	0	0	.022	.090	.143	.173	.183			
19.0	12.5	.005	.013	.035	.075	.127	.180	.220	.248	.266	.283			
21.5	12.5	.027	.081	.143	.186	.215	.236	.253	.266	.278	.288			
24.0	12.5	.056	.141	.178	.191	.193	.191	.195	.197	.199	.200			
26.5	12.5	.092	.130	.131	.130	.128	.125	.124	.122	.120	.118			
29.0	12.5	.078	.072	.065	.063	.061	.058	.055	.052	.049	.046			
34.0	12.5	-.003	-.015	-.020	-.023	-.024	-.030	-.034	-.038	-.042	-.045			
39.0	12.5	-.050	-.057	-.060	-.065	-.067	-.070	-.073	-.076	-.080	-.083			
49.0	12.5	0	-.005	-.010	-.015	-.021	-.022	-.024	-.031	-.045	-.062			
59.0	12.5	-.005	-.005	-.006	-.007	-.008	-.010	-.011	-.012	-.015	-.017			
19.0	17.5	.003	.005	.007	.008	.010	.031	.073	.102	.120	.131			
24.0	17.5	.003	.023	.062	.095	.122	.140	.156	.173	.190	.206			
26.5	17.5	.020	.073	.118	.142	.150	.159	.166	.175	.183	.191			
31.5	17.5	.072	.102	.104	.105	.104	.102	.099	.094	.089	.087			
36.5	17.5	.058	.030	.025	.023	.021	.017	.013	.010	.005	0			
41.5	17.5	-.020	-.030	-.032	-.032	-.033	-.035	-.040	-.045	-.047	-.055			
61.5	17.5	0	0	-.002	-.004	-.005	-.006	-.007	-.008	-.009	-.011			
31.5	25.0	.016	.035	.051	.063	.073	.080	.085	.088	.090	.090			
39.0	25.0	.041	.074	.075	.075	.074	.072	.070	.070	.070	.070			
54.0	25.0	-.022	-.030	-.027	-.025	-.026	-.033	-.038	-.040	-.041	-.041			
59.0	25.0	-.010	-.015	-.015	-.018	-.027	-.042	-.047	-.047	-.046	-.046			
64.0	25.0	-.010	-.017	-.020	-.024	-.027	-.031	-.035	-.035	-.035	-.036			
41.5	30.0	.031	.050	.061	.066	.070	.070	.068	.067	.065	.063			
46.5	30.0	.055	.052	.054	.055	.052	.050	.047	.047	.046	.045			
51.5	30.0	-.008	-.010	-.012	-.015	-.015	-.015	-.015	-.015	-.013	-.013			
61.5	30.0	-.015	-.023	-.027	-.030	-.031	-.032	-.032	-.032	-.032	-.031			

TABLE 4.- WING PRESSURES FOR SUPERSONIC NOZZLE ($M_j = 1.74$) AT POSITION A

Orifice ordinates		Incremental wing pressure coefficients for $p_{t,c}/p_\infty$ of -												
x/D _T	y/D _T	10	20	30	40	50	60	70	80	90	100	110	120	130
11.5	2.5			0.007	0.007	0.008	0.010	0.010	0.011	0.013	0.015	0.015	0.015	0.015
14.0	2.5	0	0	0	0	0	0	0	0.002	0.012	0.025	0.049	0.088	
19.0	2.5	0		.025	.051	.082	.125	.189	.262	.310	.339	.362	.378	
21.5	2.5	.105		.134	.340	.490	.525	.514	.480	.454	.440	.442	.448	
24.0	2.5	.580		.585	.541	.532	.528	.525	.525	.523	.519	.518	.514	
26.5	2.5	.270		.306	.280	.244	.211	.190	.176	.168	.163	.160	.159	
29.0	2.5	-.041		-.053	-.085	-.110	-.127	-.140	-.150	-.158	-.163	-.168	-.170	
34.0	2.5	-.120		-.170	-.188	-.190	-.204	-.198	-.190	-.187	-.186	-.184	-.192	
39.0	2.5	-.045		-.053	-.060	-.068	-.086	-.105	-.120	-.135	-.147	-.155	-.155	
44.0	2.5	-.030		-.034	-.040	-.043	-.047	-.051	-.056	-.062	-.068	-.075	-.085	
49.0	2.5	-.008		-.008	-.027	-.040	-.045	-.045	-.045	-.048	-.050	-.052	-.052	
54.0	2.5	-.012		-.014	-.015	-.017	-.020	-.023	-.025	-.025	-.027	-.029	-.030	
64.0	2.5	-.005		-.007	-.009	-.010	-.012	-.013	-.015	-.015	-.017	-.018	-.019	
11.5	7.5			.005	.005	.005	.005	.005	.006	.008	.009	.010	.010	
14.0	7.5	.008		.008	.008	.008	.008	.010	.010	.015	.025	.040	.065	
19.0	7.5	.012		.020	.070	.134	.195	.236	.268	.295	.317	.337	.356	
21.5	7.5	.095		.178	.234	.273	.307	.334	.354	.367	.375	.377	.375	
24.0	7.5	.233		.276	.310	.339	.366	.393	.434	.504	.596	.671	.675	
26.5	7.5	.084		.090	.104	.125	.161	.215	.264	.250	.195	.168	.138	
31.5	7.5	.055		.050	.074	.100	.107	.074	.069	-.005	-.048	-.080	-.100	
36.5	7.5	-.055		-.065	-.068	-.077	-.088	-.105	-.115	-.130	-.143	-.148	-.150	
41.5	7.5	-.060		-.083	-.100	-.116	-.124	-.125	-.100	-.073	-.065	-.068	-.078	
46.5	7.5	-.018		-.016	-.020	-.028	-.048	-.077	-.097	-.106	-.110	-.106	-.100	
51.5	7.5	-.025		-.025	-.025	-.021	-.022	-.025	-.027	-.031	-.035	-.036	-.044	
61.5	7.5	-.016		-.017	-.018	-.020	-.020	-.023	-.025	-.025	-.026	-.027	-.030	
9.0	12.5	0	0	0	0	0	0	0	0	0	0	0	0	
16.5	12.5	0	0	0	0	0	0	0	.011	.027	.037	.110		
19.0	12.5	0	0	0	0	0	.015	.055	.107	.165	.210	.242	.268	
21.5	12.5			.005	.005	.047	.115	.170	.210	.242	.269	.295	.320	.339
24.0	12.5			.070	.110	.177	.213	.231	.254	.280	.296	.300	.283	.250
26.5	12.5			.140	.164	.194	.210	.220	.220	.219	.211	.201	.203	.210
29.0	12.5			.147	.157	.170	.180	.185	.180	.177	.175	.174	.195	.240
34.0	12.5			.066	.070	.070	.065	.061	.061	.065	.069	.073	.080	.075
39.0	12.5			-.015	-.015	-.017	-.023	-.030	-.052	-.036	-.039	-.042	-.045	-.049
49.0	12.5			-.033	-.035	-.043	-.062	-.088	-.097	-.094	-.090	-.090	-.090	-.091
59.0	12.5			-.018	-.015	-.015	-.019	-.024	-.030	-.035	-.040	-.043	-.044	-.045
19.0	17.5	0	0	0	0	0	0	0	.009	.032	.067	.105	.138	
24.0	17.5			.005	.005	.019	.052	.094	.130	.160	.183	.198	.210	.220
26.5	17.5			.025	.031	.085	.126	.152	.169	.189	.206	.218	.225	.222
31.5	17.5			.090	.116	.133	.144	.149	.152	.147	.130	.100	.081	.069
36.5	17.5			.093	.097	.098	.092	.082	.070	.063	.060	.060	.065	
41.5	17.5			.025	.029	.030	.025	.017	.010	.007	.005	.005	.005	.005
61.5	17.5			-.037	-.041	-.050	-.049	-.053	-.057	-.061	-.067	-.068	-.072	-.075
31.5	25.0			.005	.008	.020	.040	.066	.085	.095	.103	.107	.110	.110
39.0	25.0			.036	.070	.090	.100	.106	.107	.105	.104	.100	.090	
54.0	25.0			.012	.015	.018	.014	.006	-.002	-.006	-.005	-.006	-.006	
59.0	25.0			-.008	-.005	-.009	-.016	-.023	-.025	-.026	-.029	-.030	-.030	-.030
64.0	25.0			-.026	-.027	-.055	-.042	-.048	-.050	-.055	-.056	-.057	-.057	-.054
41.5	30.0				.025	.020	.038	.055	.067	.074	.075	.075	.071	.066
46.5	30.0				.050	.063	.073	.078	.078	.078	.078	.076	.075	.073
51.5	30.0				.035	.035	.046	.055	.055	.055	.050	.049	.043	.025
61.5	30.0				.008	.013	.015	.015	.009	.004	0	-.004	-.005	-.006

TABLE 5.- WING PRESSURES FOR SUPERSONIC NOZZLE ($M_j = 1.74$) AT POSITION B

Orifice ordinates		Incremental wing pressure coefficients for $p_{t,c}/p_\infty$ of -												
x/D_T	y/D_T	10	20	30	40	50	60	70	80	90	100	110	120	130
11.5	2.5			0	0	0	0	0	0.002	0.007	0.015	0.028	0.040	
14.0	2.5			.006	.010	.013	.022	.048	.092	.145	.199	.241	.267	
19.0	2.5			.160	.215	.272	.324	.358	.382	.400	.414	.425	.435	
21.5	2.5			.285	.300	.320	.337	.344	.354	.359	.368	.370	.370	
24.0	2.5			.195	.194	.196	.200	.202	.204	.205	.205	.205	.205	
26.5	2.5			.090	.079	.078	.076	.075	.077	.075	.074	.073	.073	
29.0	2.5			-.005	-.010	-.011	-.013	-.015	-.017	-.015	-.015	-.015	-.015	
34.0	2.5			-.115	-.118	-.124	-.137	-.142	-.144	-.149	-.150	-.152	-.153	
39.0	2.5			-.027	-.039	-.039	-.040	-.049	-.051	-.067	-.082	-.015	-.119	
44.0	2.5			-.015	-.018	-.028	-.026	-.020	-.023	-.029	-.034	-.035	-.039	
49.0	2.5			-.013	-.013	-.015	-.016	-.017	-.018	-.019	-.020	-.020	-.020	
54.0	2.5			-.015	-.016	-.017	-.018	-.020	-.020	-.020	-.020	-.021	-.021	
64.0	2.5			-.015	-.015	-.015	-.015	-.015	-.015	-.015	-.015	-.015	-.015	
11.5	7.5			0	0	0	0	0	0	0	0	0	0	
14.0	7.5			0	0	0	0	0	.012	.045	.096	.139	.166	
19.0	7.5			.150	.160	.188	.218	.248	.277	.307	.335	.369	.392	
21.5	7.5			.185	.220	.257	.300	.341	.381	.420	.455	.485	.509	
24.0	7.5			.250	.260	.285	.310	.325	.335	.339	.345	.349	.350	
26.5	7.5			.071	.072	.072	.072	.072	.072	.071	.069	.065	.060	
31.5	7.5			-.022	-.030	-.035	-.040	-.046	-.051	-.057	-.061	-.066	-.066	
36.5	7.5			-.105	-.107	-.108	-.115	-.121	-.126	-.131	-.137	-.143	-.150	
41.5	7.5			-.028	-.025	-.029	-.046	-.073	-.100	-.118	-.125	-.125	-.125	
46.5	7.5			-.018	-.018	-.019	-.020	-.020	-.021	-.022	-.023	-.030	-.045	
51.5	7.5			-.004	-.009	-.010	-.011	-.010	-.010	-.007	-.005	-.003	0	
61.5	7.5			-.013	-.014	-.014	-.015	-.015	-.015	-.015	-.016	-.016	-.016	
9.0	12.5			0	0	0	0	0	0	0	0	0	0	
16.5	12.5			0	0	0	.007	.035	.080	.123	.150	.172	.187	
19.0	12.5			.040	.020	.064	.110	.145	.161	.175	.176	.170	.160	
21.5	12.5			.137	.170	.200	.217	.220	.218	.217	.225	.247	.280	
24.0	12.5			.095	.110	.122	.136	.153	.172	.200	.232	.272	.335	
26.5	12.5			.118	.145	.168	.190	.212	.235	.258	.279	.295	.310	
29.0	12.5			.100	.120	.135	.145	.153	.151	.159	.160	.159	.155	
34.0	12.5			.031	.025	.021	.017	.012	.005	-.002	-.009	-.014	-.017	
39.0	12.5			-.060	-.062	-.065	-.067	-.070	-.075	-.086	-.092	-.096	-.100	
49.0	12.5			-.015	-.017	-.019	-.023	-.032	-.050	-.065	-.080	-.092	-.102	
59.0	12.5			0	-.005	-.007	-.006	-.005	-.005	-.005	-.004	-.003	-.002	
19.0	17.5			.002	.003	.005	.008	.034	.090	.141	.171	.190	.202	
24.0	17.5			.058	.069	.097	.123	.133	.135	.132	.125	.113	.100	
26.5	17.5			.092	.100	.115	.120	.120	.117	.115	.120	.126	.145	
31.5	17.5			.093	.095	.098	.100	.107	.115	.128	.140	.150	.175	
36.5	17.5			.042	.047	.054	.059	.062	.064	.065	.065	.065	.063	
41.5	17.5			-.003	-.005	-.008	-.010	-.014	-.017	-.020	-.025	-.029	-.032	
61.5	17.5			-.011	-.012	-.012	-.012	-.013	-.012	-.011	-.010	-.010	-.010	
31.5	25.0			.075	.080	.094	.099	.116	.120	.123	.125	.125	.126	
39.0	25.0			.066	.073	.075	.075	.075	.074	.070	.065	.060	.055	
54.0	25.0			-.025	-.024	-.020	-.019	-.027	-.035	-.035	-.036	-.036	-.035	
59.0	25.0			-.045	-.040	-.034	-.041	-.049	-.050	-.052	-.054	-.055	-.056	
64.0	25.0			-.022	-.020	-.021	-.024	-.027	-.035	-.038	.042	-.045	-.045	
41.5	30.0			.088	.083	.080	.085	.092	.094	.094	.091	.090	.090	
46.5	30.0			.056	.055	.055	.056	.058	.059	.055	.054	.059	.060	
51.5	30.0			.050	.051	.050	.029	.025	.026	.021	.019	.019	.018	
61.5	30.0			-.033	-.034	-.030	-.025	-.024	-.028	-.030	-.034	-.035	-.035	

L-1614

TABLE 6.- WING PRESSURES FOR SUPERSONIC NOZZLE ($M_j = 1.74$) AT POSITION C

Orifice ordinates		Incremental wing pressure coefficients for $p_{t,c}/p_\infty$ of -												
x/D _T	y/D _T	10	20	30	40	50	60	70	80	90	100	110	120	130
11.5	2.5	0.005	0.005	0.005	0.006	0.008	0.020	0.050	0.090	0.116	0.145			
14.0	2.5	0	0	0	.025	.085	.125	.170	.255	.310	.345			
19.0	2.5	.159	.240	.255	.265	.269	.275	.280	.277	.275	.273			
21.5	2.5	.140	.150	.154	.160	.165	.163	.160	.155	.150	.151			
24.0	2.5	.080	.084	.085	.085	.088	.085	.081	.075	.073	.071			
26.5	2.5	.010	.011	.013	.013	.010	.007	.004	.001	-.001	-.002			
29.0	2.5	-.033	-.035	-.036	-.037	-.040	-.044	-.047	-.050	-.052	-.053			
34.0	2.5	-.068	-.073	-.078	-.082	-.093	-.100	-.103	-.108	-.108	-.110			
39.0	2.5	-.025	-.025	-.025	-.024	-.029	-.042	-.080	-.107	-.125	-.142			
44.0	2.5	-.020	-.019	-.018	-.017	-.021	-.029	-.030	-.041	-.035	-.038			
49.0	2.5													
54.0	2.5	-.007	-.006	-.005	-.005	-.005	-.005	-.005	-.005	-.005	-.005	-.007		
64.0	2.5	-.005	-.005	-.005	-.005	-.005	-.005	-.005	-.005	-.005	-.005	-.005		
11.5	7.5	0	0	0	0	0	.002	.005	.007	.020	.057			
14.0	7.5	0	0	0	0	.013	.060	.128	.191	.235	.271			
19.0	7.5	.105	.160	.202	.231	.262	.274	.287	.289	.301	.307			
21.5	7.5	.123	.183	.197	.202	.207	.209	.214	.217	.217	.219			
24.0	7.5	.116	.122	.122	.122	.124	.124	.127	.120	.122	.127			
26.5	7.5	.025	.025	.025	.025	.025	.023	.021	.019	.017	.016			
31.5	7.5	-.036	-.039	-.041	-.044	-.047	-.055	-.062	-.066	-.070	-.071			
36.5	7.5	-.054	-.057	-.061	-.072	-.075	-.088	-.092	-.095	-.099	-.102			
41.5	7.5	-.020	-.020	-.020	-.022	-.043	-.071	-.091	-.106	-.100	-.104			
46.5	7.5	-.014	-.015	-.015	-.015	-.018	-.025	-.027	-.026	-.023	-.025			
51.5	7.5	-.010	-.010	-.010	-.010	-.013	-.019	-.019	-.019	-.015	-.015			
61.5	7.5	-.007	-.007	-.006	-.005	-.005	-.006	-.005	-.007	-.007	-.007			
9.0	12.5	0	0	0	0	0	0	0	0	0	0			
16.5	12.5	0	0	0	0	0	.045	.105	.155	.180	.205			
19.0	12.5	0	0	.005	.055	.154	.195	.225	.255	.280	.297			
21.5	12.5	.079	.126	.164	.198	.234	.249	.260	.265	.279	.289			
24.0	12.5	.098	.153	.181	.193	.195	.197	.195	.193	.193	.197			
26.5	12.5	.110	.129	.120	.127	.124	.119	.117	.113	.110	.109			
29.0	12.5	.070	.067	.062	.065	.060	.057	.051	.045	.045	.042			
34.0	12.5	-.016	-.019	-.020	-.026	-.032	-.040	-.045	-.050	-.055	-.056			
39.0	12.5	-.035	-.044	-.050	-.060	-.069	-.075	-.078	-.085	-.086	-.089			
49.0	12.5	-.003	-.005	-.006	-.007	-.015	-.025	-.043	-.067	-.081	-.090			
59.0	12.5	-.010	-.010	-.010	-.010	-.012	-.013	-.013	-.016	-.014	-.013			
19.0	17.5	0	0	0	0	.017	.044	.080	.105	.119	.130			
24.0	17.5	.020	.040	.070	.101	.136	.150	.165	.175	.190	.209			
26.5	17.5	.053	.096	.125	.142	.155	.160	.167	.174	.180	.189			
31.5	17.5	.079	.094	.094	.098	.096	.094	.089	.084	.082	.080			
36.5	17.5	.026	.023	.021	.021	.015	.014	.007	0	-.005	-.007			
41.5	17.5	-.035	-.036	-.035	-.039	-.045	-.050	-.053	-.057	-.062	-.065			
61.5	17.5	-.005	-.007	-.009	-.010	-.012	-.014	-.015	-.016	-.016	-.016			
31.5	25.0	----	----	----	----	----	----	----	----	----	----			
39.0	25.0	.053	.068	.069	.074	.074	.070	.068	.065	.065	.066			
54.0	25.0	-.043	-.040	-.031	-.027	-.030	-.044	-.049	-.050	-.050	-.050			
59.0	25.0	-.045	-.043	-.040	-.035	-.041	-.050	-.051	-.052	-.052	-.052			
64.0	25.0	----	----	----	----	----	----	----	----	----	----			
41.5	30.0	----	----	----	----	----	----	----	----	----	----			
46.5	30.0	.045	.050	.048	.045	.045	.046	.045	.045	.045	.045			
51.5	30.0	----	----	----	----	----	----	----	----	----	----			
61.5	30.0	-.010	-.018	-.025	-.030	-.033	-.035	-.035	-.036	-.038	-.040			

TABLE 7.- WING PRESSURES FOR SUPERSONIC NOZZLE ($M_j = 3.04$) AT POSITION A

Orifice ordinates		Incremental wing pressure coefficients for $p_{t,c}/p_\infty$ of -												
x/D_T	y/D_T	10	20	30	40	50	60	70	80	90	100	110	120	130
11.5	2.5	0	0	0	0	0	0	0	0	0	0	0	0	0
14.0	2.5	0	0	0	0	0	0	0	0	0	0	0	0	0
19.0	2.5	.005	.015	.001	.015	.042	.061	.074	.106	.160	.246			
21.5	2.5	.003	.023	.043	.071	.156	.383	.459	.488	.488	.471			
24.0	2.5	.115	.277	.435	.586	.525	.506	.495	.494	.490	.500			
26.5	2.5	.211	.439	.385	.325	.287	.257	.240	.210	.195	.190			
29.0	2.5	0	0	0	0	0	0	0	0	0	0	0	0	0
34.0	2.5	-.050	-.097	-.137	-.168	-.193	-.208	-.220	-.230	-.245	-.254			
39.0	2.5	-.003	-.012	-.025	-.040	-.059	-.077	-.095	-.112	-.127	-.140			
44.0	2.5	-.007	-.012	-.018	-.026	-.038	-.055	-.070	-.083	-.090	-.095			
49.0	2.5	----	----	----	----	----	----	----	----	----	----			
54.0	2.5	-.005	-.007	-.009	-.010	-.014	-.017	-.019	-.020	-.023	-.025			
64.0	2.5	-.002	-.002	-.005	-.008	-.010	-.014	-.014	-.012	-.011	-.010			
11.5	7.5	0	0	0	0	0	0	0	0	0	0	0	0	0
14.0	7.5	.004	.004	.004	.004	-.001	-.006	-.006	-.006	-.006	-.006	-.006	-.006	-.006
19.0	7.5	0	.003	.005	.009	.043	.098	.150	.195	.230	.252			
21.5	7.5	.007	.020	.066	.141	.204	.247	.277	.299	.324	.348			
24.0	7.5	.036	.126	.206	.265	.300	.323	.348	.371	.393	.416			
26.5	7.5	.040	.070	.085	.095	.107	.129	.155	.200	.244	.265			
31.5	7.5	.007	.022	.042	.069	.112	.160	.165	.075	-.020	-.100			
36.5	7.5	-.025	-.045	-.062	-.070	-.077	-.084	-.100	-.130	-.172	-.225			
41.5	7.5	-.020	-.042	-.065	-.087	-.110	-.128	-.146	-.162	-.175	-.182			
46.5	7.5	-.012	-.017	-.016	-.018	-.026	-.039	-.050	-.059	-.062	-.065			
51.5	7.5	-.011	-.017	-.019	-.019	-.020	-.025	-.026	-.026	-.025	-.022			
61.5	7.5	-.005	-.017	-.017	-.017	-.017	-.019	-.020	-.020	-.020	-.020			
9.0	12.5	0	0	0	0	0	0	0	0	0	0	0	0	0
16.5	12.5	0	0	0	0	0	0	0	0	0	0	0	0	0
19.0	12.5	0	0	0	0	0	0	0	0	0	0	0	0	0
21.5	12.5	0	0	0	0	.005	.030	.092	.142	.184	.216	.242		
24.0	12.5	.012	.020	.033	.095	.165	.198	.220	.242	.261	.280			
26.5	12.5	.015	.056	.118	.164	.192	.213	.228	.239	.246	.253			
29.0	12.5	.034	.090	.134	.157	.170	.179	.185	.190	.192	.195			
34.0	12.5	.050	.076	.075	.074	.075	.075	.077	.085	.099	.115			
39.0	12.5	.018	.005	-.009	-.015	-.019	-.022	-.025	-.026	-.028	-.030			
49.0	12.5	-.017	-.030	-.040	-.049	-.064	-.084	-.102	-.114	-.122	-.128			
59.0	12.5	-.006	-.011	-.014	-.015	-.016	-.020	-.022	-.026	-.030	-.035			
19.0	17.5	0	0	0	0	0	0	0	0	0	0	0	0	0.010
24.0	17.5	0	0	.004	.005	.010	.034	.074	.114	.147	.162			
26.5	17.5	0	.004	.005	.025	.076	.118	.147	.170	.185	.196			
31.5	17.5	.006	.035	.077	.111	.130	.144	.150	.152	.155	.155			
36.5	17.5	.022	.059	.085	.095	.095	.095	.094	.091	.088	.085			
41.5	17.5	.012	.025	.024	.021	.020	.018	.015	.010	.009	.008			
61.5	17.5	-.007	-.011	-.015	-.020	-.023	-.027	-.031	-.035	-.039	-.044			
31.5	25.0	.005	.020	.043	.065	.085	.095	.103	.105	.108	.108			
39.0	25.0	.007	.012	.015	.015	.014	.011	.009	.004	0	-.005			
54.0	25.0	-.006	-.012	-.015	-.018	-.020	-.023	-.025	-.026	-.027	-.030			
64.0	25.0													
41.5	30.0	.028	.045	.055	.060	.072	.078	.083	.084	.086	.086			
46.5	30.0													
51.5	30.0	.010	.015	.015	.015	.013	.009	.005	0	0	0			
61.5	30.0													

L-1614

TABLE 8.- WING PRESSURES FOR SUPERSONIC NOZZLE ($M_j = 3.04$) AT POSITION C

Orifice ordinates		Incremental wing pressure coefficients for $P_{t,c}/P_\infty$ of -												
x/D_T	y/D_T	10	20	30	40	50	60	70	80	90	100	110	120	130
11.5	2.5	0	0	0	.005	.005	.005	.011	.028	.066	.116	.158	.188	
14.0	2.5	0	0	0	.005	.016	.042	.110	.175	.229	.280	.325	.370	
19.0	2.5	.057	.116	.175	.228	.268	.287	.301	.315	.324	.328	.327	.325	
21.5	2.5	.100	.147	.178	.200	.207	.205	.205	.205	.204	.199	.194	.191	
24.0	2.5	.090	.107	.115	.115	.115	.115	.111	.109	.106	.101	.100	.100	
26.5	2.5	.058	.060	.060	.055	.054	.050	.048	.045	.040	.035	.033	.030	
29.0	2.5	.011	.013	.007	-.001	-.007	-.010	-.015	-.020	-.025	-.027	-.030	-.035	
34.0	2.5	-.040	-.064	-.077	-.085	-.087	-.090	-.094	-.095	-.097	-.100	-.098	-.100	
39.0	2.5	-.016	-.018	-.024	-.027	-.047	-.098	-.115	-.126	-.135	-.143	-.146	-.149	
44.0	2.5	-.014	-.020	-.024	-.024	-.025	-.026	-.030	-.033	-.035	-.040	-.048	-.057	
49.0	2.5	-.010	-.013	-.017	-.020	-.025	-.027	-.030	-.033	-.035	-.035	-.036	-.038	
54.0	2.5	-.009	-.010	-.012	-.012	-.010	-.010	-.010	-.008	-.007	-.010	-.015	-.017	
64.0	2.5	-.005	-.005	-.005	-.005	-.005	-.005	-.005	-.005	-.005	-.005	-.005	-.005	
11.5	7.5	.005	.007	.007	.007	.007	.007	.007	.007	.006	.022	.052	.113	
14.0	7.5	.004	.006	.007	.007	.006	.005	.032	.090	.162	.210	.250	.285	
19.0	7.5	.038	.076	.133	.220	.273	.300	.315	.326	.337	.345	.350	.356	
21.5	7.5	.068	.150	.200	.227	.238	.241	.245	.245	.247	.247	.245	.245	
24.0	7.5	.112	.148	.155	.159	.160	.160	.155	.154	.150	.146	.143	.138	
26.5	7.5	.026	.030	.032	.032	.030	.029	.026	.025	.020	.019	.016	.015	
31.5	7.5	-.010	-.017	-.021	-.025	-.027	-.031	-.035	-.040	-.044	-.048	-.054	-.057	
36.5	7.5	-.055	-.066	-.072	-.083	-.090	-.096	-.100	-.105	-.107	-.110	-.113	-.115	
41.5	7.5	-.014	-.015	-.017	-.019	-.042	-.087	-.105	-.111	-.118	-.124	-.125	-.125	
46.5	7.5	-.014	-.015	-.018	-.022	-.024	-.025	-.025	-.026	-.036	-.063	-.090	-.109	
51.5	7.5	-.011	-.015	-.013	-.013	-.013	-.014	-.015	-.015	-.015	-.016	-.018	-.020	
61.5	7.5	-.004	-.004	-.004	-.004	-.004	-.004	-.004	-.004	-.004	-.004	-.004	-.004	
9.0	12.5	0	0	0	0	0	0	0	0	0	0	0	0	
16.5	12.5	0	0	0	0	.005	.041	.102	.148	.176	.198	.220	.240	
19.0	12.5	0	.002	.003	.013	.094	.165	.209	.235	.262	.289	.316	.343	
21.5	12.5	.028	.050	.087	.162	.218	.248	.270	.289	.303	.316	.325	.336	
24.0	12.5	.070	.132	.182	.207	.220	.226	.231	.235	.236	.236	.235	.234	
26.5	12.5	.097	.143	.154	.155	.152	.153	.150	.145	.143	.140	.136	.132	
29.0	12.5	.085	.090	.087	.083	.077	.073	.068	.064	.060	.059	.056	.051	
34.0	12.5	.011	.005	-.001	-.005	-.010	-.016	-.020	-.025	-.029	-.033	-.036	-.040	
39.0	12.5	-.044	-.051	-.055	-.060	-.064	-.067	-.072	-.075	-.078	-.081	-.084	-.086	
49.0	12.5	-.005	-.007	-.010	-.011	-.012	-.020	-.020	-.024	-.027	-.103	-.115	-.123	
59.0	12.5	-.005	-.005	-.005	-.005	-.005	-.005	-.005	-.005	-.005	-.005	-.005	-.005	
19.0	17.5	0	0	.002	.004	.025	.062	.094	.116	.132	.142	.150	.155	
24.0	17.5	.002	.007	.015	.080	.125	.146	.162	.181	.200	.221	.243	.265	
26.5	17.5	.022	.052	.092	.138	.154	.167	.180	.191	.205	.214	.221	.227	
31.5	17.5	.065	.100	.106	.109	.109	.108	.105	.103	.100	.098	.094	.090	
36.5	17.5	.045	.040	.035	.030	.025	.020	.015	.012	.009	.005	.003	0	
41.5	17.5	-.023	-.030	-.037	-.044	-.050	-.055	-.056	-.060	-.063	-.065	-.069	-.071	
61.5	17.5	-.004	-.005	-.005	-.005	-.006	-.007	-.010	-.011	-.016	-.025	-.033	-.040	
31.5	25.0	.025	.025	.030	.058	.098	.110	.106	.109	.120	.125	.130	.131	
39.0	25.0	.045	.072	.080	.078	.079	.077	.076	.075	.075	.075	.075	.075	
54.0	25.0	-.015	-.024	-.030	-.035	-.039	-.042	-.045	-.050	-.055	-.058	-.059	-.060	
59.0	25.0	-.010	-.021	-.030	-.042	-.049	-.055	-.058	-.060	-.060	-.060	-.060	-.060	
64.0	25.0	-.014	-.016	-.015	-.017	-.020	-.024	-.031	-.040	-.045	-.047	-.049	-.050	
41.5	30.0	.025	.035	.056	.074	.075	-.075	-.075	.074	.071	.070	.070	.070	
46.5	30.0	.050	.052	.052	.052	.050	.050	.050	.049	.048	.046	.045	.044	
51.5	30.0	.015	.015	.014	.017	.020	.017	.013	.010	.005	.004	0	0	
61.5	30.0	-.024	-.025	-.029	-.033	-.035	-.040	-.045	-.046	-.047	-.049	-.050	-.050	

TABLE 9.- WING PRESSURES FOR TWO-DIMENSIONAL SUPERSONIC NOZZLE ($M_j = 1.71$) AT POSITION A

Orifice ordinates		Incremental wing pressure coefficients for $P_t, c/p_\infty$ of -												
x/D _T	y/D _T	10	20	30	40	50	60	70	80	90	100	110	120	130
11.5	2.5	0	0	0	0	0	0	0	0	0	0	0	0	0
14.0	2.5	0	0	0	0	0	0	0	0	0	0	0	0	0
19.0	2.5	.008	.035	.075	.120	.162	.208							
21.5	2.5	.058	.145	.207	.261	.310	.355							
24.0	2.5	.175	.303	.390	.412	.525	.588							
26.5	2.5	.220	.300	.330	.328	.326	.325							
29.0	2.5	.025	.020	-.006	-.040	-.075	-.114							
34.0	2.5	-.082	-.130	-.160	-.186	-.243	-.260							
39.0	2.5	-.036	-.045	-.047	-.050	-.055	-.056							
44.0	2.5	-.024	-.031	-.030	-.034	-.043	-.055							
49.0	2.5	-.023	-.030	-.034	-.037	-.040	-.040							
54.0	2.5	-.016	-.020	-.020	-.025	-.033	-.036							
64.0	2.5	-.005	-.008	-.009	-.013	-.015	-.020							
11.5	7.5	-.005	-.006	-.006	-.005	-.005	-.005							
14.0	7.5	-.010	-.010	-.010	-.010	-.010	-.010							
19.0	7.5	-.014	-.013	-.010	.011	.065	.141							
21.5	7.5	-.010	.022	.088	.150	.192	.227							
24.0	7.5	.052	.140	.186	.202	.250	.279							
26.5	7.5	.013	.054	.076	.090	.105	.128							
31.5	7.5	.088	.088	.090	.105	.121	.115							
36.5	7.5	-.080	-.085	-.085	-.082	-.094	-.112							
41.5	7.5	-.055	-.075	-.087	-.104	-.130	-.171							
46.5	7.5	-.018	-.023	-.021	-.019	-.025	-.036							
51.5	7.5	-.025	-.030	-.030	-.035	-.039	-.042							
61.5	7.5	-.010	-.015	-.020	-.024	-.030	-.035							
9.0	12.5	0	0	0	0	0	0							
16.5	12.5	0	0	0	0	0	0							
19.0	12.5	0	0	0	0	0	0							
21.5	12.5	0	0	0	.021	.086	.156							
24.0	12.5	.002	.025	.068	.123	.158	.184							
26.5	12.5	.050	.106	.127	.142	.154	.163							
29.0	12.5	.086	.121	.125	.125	.125	.125							
34.0	12.5	.082	.087	.084	.091	.105	.122							
39.0	12.5	.020	.013	.011	.010	.012	.015							
49.0	12.5	-.028	-.046	-.052	-.055	-.065	-.080							
59.0	12.5	-.010	-.014	-.015	-.020	-.025	-.030							
19.0	17.5	0	0	0	0	0	0							
24.0	17.5	0	0	0	.010	.054	.118							
26.5	17.5	0	0	.024	.070	.109	.138							
31.5	17.5	.018	.060	.093	.105	.102	.099							
36.5	17.5	.040	.068	.071	.066	.060	.050							
41.5	17.5	0	0	0	0	0	0							
61.5	17.5	-.007	-.012	-.017	-.020	-.020	-.021							
31.5	25.0	0	.002	.005	.025	.076	.016							
39.0	25.0	.009	.037	.052	.065	.070	.075							
54.0	25.0	.005	.008	.009	.007	.005	.002							
59.0	25.0	-.010	-.015	-.017	-.020	-.021	-.023							
64.0	25.0	-.015	-.023	-.027	-.031	-.035	-.035							
41.5	30.0	.010	.022	.035	.056	.074	.086							
46.5	30.0	.027	.044	.050	.060	.065	.066							
51.5	30.0	.030	.035	.042	.044	.043	.039							
61.5	30.0	.005	.005	.005	.003	-.002	-.006							

TABLE 10.- WING PRESSURES FOR TWO-DIMENSIONAL SUPERSONIC NOZZLE ($M_j = 1.71$) AT POSITION B

Orifice ordinates		Incremental wing pressure coefficients for $p_{t,c}/p_\infty$ of -												
x/D_T	y/D_T	10	20	30	40	50	60	70	80	90	100	110	120	130
11.5	2.5	0	0	0	0	0	0							
14.0	2.5	0	0	0	.015	.044	.080							
19.0	2.5	0	.082	.182	.280	.355	.420							
21.5	2.5	.065	.160	.325	.306	.280	.295							
24.0	2.5	.114	.142	.148	.153	.156	.152							
26.5	2.5	.050	.050	.038	.032	.024	.015							
29.0	2.5	-.003	-.022	-.034	-.041	-.050	-.056							
34.0	2.5	-.021	-.055	-.085	-.107	-.125	-.137							
39.0	2.5	-.014	-.030	-.035	-.032	-.046	-.040							
44.0	2.5	-.012	-.018	-.020	-.021	-.021	-.018							
49.0	2.5	-.011	-.013	-.014	-.015	-.015	-.016							
54.0	2.5	-.006	0	-.008	-.011	-.010	-.006							
64.0	2.5	.006	0	-.009	-.010	-.012	-.015							
11.5	7.5	0	0	0	0	0	0							
14.0	7.5	0	0	0	0	0	0							
19.0	7.5	0	.017	.115	.203	.260	.306							
21.5	7.5	.018	.120	.224	.279	.314	.338							
24.0	7.5	.062	.166	.230	.244	.249	.251							
26.5	7.5	.034	.047	.048	.049	.049	.045							
31.5	7.5	0	-.006	-.024	-.039	-.049	-.056							
36.5	7.5	-.033	-.076	-.105	-.107	-.110	-.126							
41.5	7.5	-.007	-.020	-.026	-.031	-.041	-.051							
46.5	7.5	0	-.011	-.021	-.026	-.029	-.030							
51.5	7.5	0	0	0	-.001	-.005	-.006							
61.5	7.5	-.002	-.005	-.010	-.012	-.013	-.015							
9.0	12.5	0	0	0	0	0	0							
16.5	12.5	0	0	0	0	0	0							
19.0	12.5	0	0	0	.003	.060	.137							
21.5	12.5	0	0	.056	.135	.197	.230							
24.0	12.5	0	.077	.163	.210	.240	.259							
26.5	12.5	.015	.125	.185	.204	.217	.223							
29.0	12.5	.050	.108	.130	.133	.135	.135							
34.0	12.5	.041	.028	.016	.007	-.002	-.013							
39.0	12.5	-.023	-.040	-.051	-.054	-.059	-.065							
49.0	12.5	0	-.015	-.025	-.030	-.040	-.055							
59.0	12.5	-.009	-.014	-.015	-.015	-.014	-.012							
19.0	17.5	0	0	0	0	0	.005							
24.0	17.5	0	0	.010	.054	.111	.136							
26.5	17.5	0	.007	.077	.132	.156	.169							
31.5	17.5	.020	.095	.125	.133	.140	.145							
36.5	17.5	.055	.069	.066	.062	.060	.056							
41.5	17.5	.023	.011	0	-.003	-.010	-.018							
61.5	17.5	0	-.007	-.015	-.017	-.020	-.023							
31.5	25.0	.007	.015	.025	.047	.073	.090							
39.0	25.0	.005	.053	.082	.087	.090	.092							
54.0	25.0	.017	.018	.010	-.007	-.019	-.021							
59.0	25.0	-.011	-.026	-.035	-.040	-.045	-.050							
64.0	25.0	-.025	-.034	-.030	-.025	-.025	-.033							
41.5	30.0	.060	.070	.070	.070	.075	.080							
46.5	30.0	.028	.048	.059	.065	.067	.070							
51.5	30.0	.023	.029	.030	.032	.030	.019							
61.5	30.0	.009	.002	-.003	-.007	-.009	-.015							

TABLE 11.- VERTICAL-STRUT PRESSURES FOR SONIC NOZZLE

Orifice ordinates		Incremental vertical strut pressure coefficients for $p_{t,c}/p_\infty$ of -												
x/p_T	z/p_T	10	20	30	40	50	60	70	80	90	100	110	120	130
(a) Position A														
29	4.05	-0.216	-0.218	-0.225	-0.240	-0.260	-0.295	-0.317						
39	4.05	-.050	-.050	-.050	-.050	-.050	-.050	-.050						
49	4.05	-.030	-.030	-.030	-.030	-.030	-.030	-.030						
22.25	8.0	.228	.213	.195	.175	.157	.135	.115						
32.25	8.0	-.126	-.141	-.153	-.167	-.181	-.195	-.208						
42.25	8.0	-.066	-.066	-.069	-.075	-.080	-.075	-.075						
15.5	12	0	0	0	0	0	0	0						
25.5	12	.152	.146	.160	.185	.189	.189	.189						
35.5	12	-.025	-.025	-.025	-.025	-.025	-.025	-.025						
(b) Position B														
29	4.05	0.05	-0.042	-0.066	-0.110	-0.120	-0.125	-0.127						
39	4.05	-.050	-.040	-.041	-.050	-.051	-.060	-.067						
49	4.05	-.015	-.015	-.015	-.015	-.017	-.019	-.022						
22.25	8.0	-.150	-.234	-.252	-.245	-.244	-.250	-.259						
32.25	8.0	-.003	.029	.045	.048	.045	.045	.046						
42.25	8.0	-.021	-.023	-.026	-.026	-.031	-.030	-.035						
15.5	12	.153	.176	.204	.215	.219	.221	.206						
25.5	12	-.110	-.110	-.110	-.110	-.110	-.110	-.110						
35.5	12	.025	.017	.012	.015	.024	.024	.029						
(c) Position C														
29	4.05	0.014	-0.001	-0.011	-0.020	-0.036	-0.058	-0.066						
39	4.05	-.052	-.044	-.045	-.047	-.050	-.057	-.068						
49	4.05	-.001	-.003	-.004	-.005	-.010	-.011	-.014						
22.25	8.0	-.017	-.030	-.037	-.045	-.057	-.097	-.120						
32.25	8.0	-.023	.025	.025	.025	.024	.023	.023						
42.25	8.0	-.012	-.015	-.017	-.019	-.020	-.023	-.025						
15.5	12	-.144	-.251	-.290	-.302	-.305	-.318	-.328						
25.5	12	-.010	-.015	-.010	-.009	-.027	-.027	-.027						
35.5	12	.017	.024	.025	.025	.025	.025	.020						

TABLE 12.- VERTICAL-STRUT PRESSURES FOR SUPERSONIC NOZZLE ($M = 1.74$)

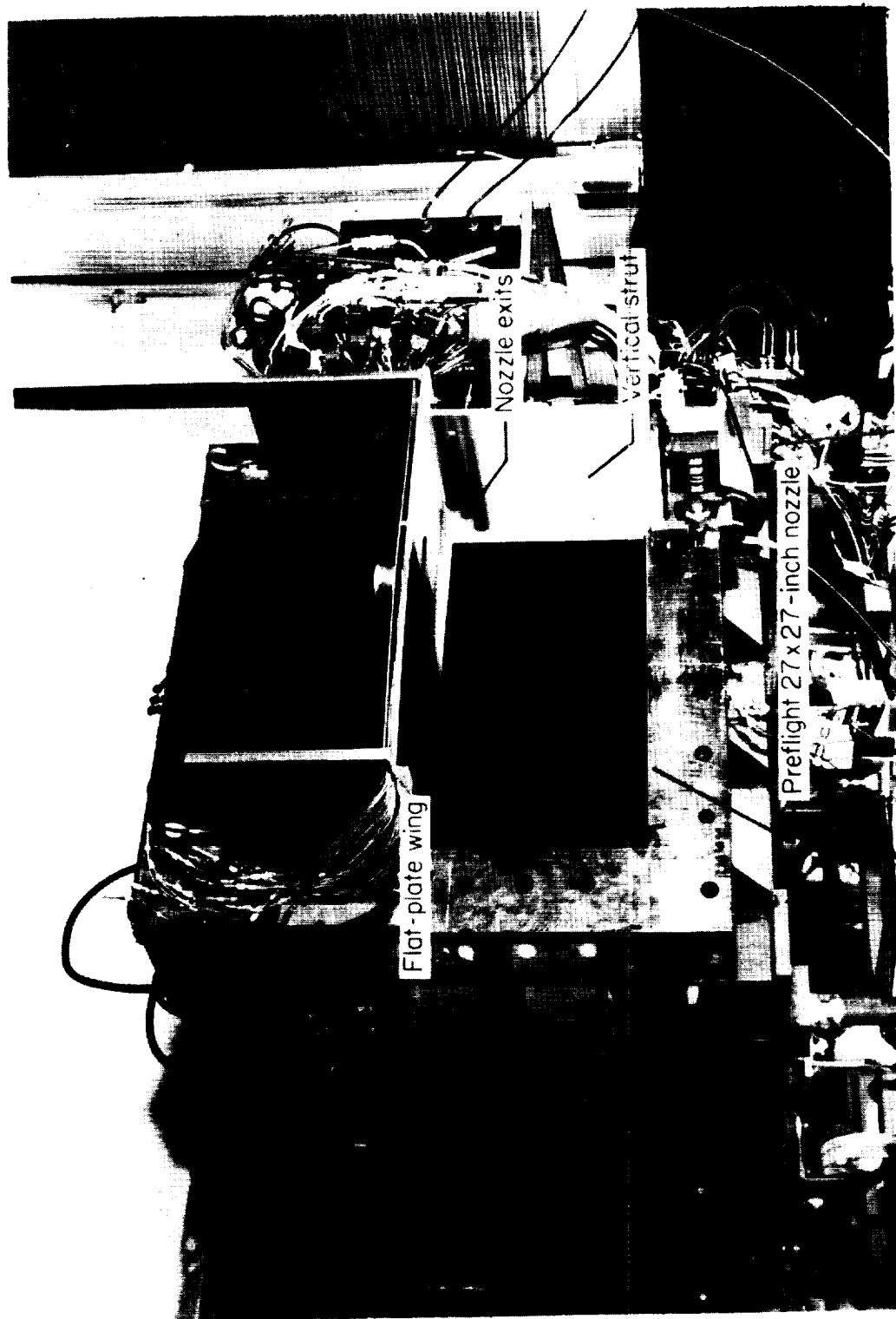
Orifice ordinates		Incremental vertical strut pressure coefficients for $P_{t,c}/P_\infty$ of -												
x/D_T	z/D_T	10	20	30	40	50	60	70	80	90	100	110	120	130
(a) Position A														
29	4.05	-0.189	-0.213	-0.226	-0.236	-0.250	-0.268	-0.287	-0.298	-0.305	-0.306			
39	4.05	-.040	-.052	-.056	-.060	-.065	-.075	-.082	-.092	-.098	-.099			
49	4.05	-.006	-.006	-.008	-.010	-.010	-.012	-.015	-.018	-.023	-.030			
22.25	8.0	.131	.180	.205	.200	.175	.151	.157	.183	.220	.265			
32.25	8.0	-.088	-.107	-.131	-.140	-.156	-.172	-.187	-.195	-.200	.205	.320		
42.25	8.0	-.020	-.030	-.030	-.022	-.010	-.005	-.004	-.006	-.016	-.027	.206		
15.5	12	-.005	-.005	-.005	-.005	-.005	-.005	-.005	-.005	-.005	-.005	.056		
25.5	12	.110	.115	.138	.141	.135	.115	.101	.105	.120	.150	.182		
35.5	12	-.027	-.027	-.027	-.027	-.028	-.029	-.030	-.032	-.036	-.040	-.045		
(b) Position B														
29	4.05	-0.010	-0.010	-0.013	-0.014	-0.014	-0.018	-0.022	-0.022	-0.025	-0.027	-0.029		
39	4.05	-.046	-.050	-.057	-.061	-.066	-.072	-.077	-.083	-.090	-.097	-.099		
49	4.05	-.020	-.022	-.025	-.025	-.026	-.026	-.027	-.030	-.031	-.035	-.035		
22.25	8.0	.183	.205	.213	.215	.220	.228	.240	.260	.268	.270			
32.25	8.0	-.048	-.045	-.037	-.040	-.058	-.086	-.115	.130	.135	.135			
42.25	8.0	-.027	-.027	-.025	-.025	-.025	-.024	-.024	-.020	-.017	-.014			
15.5	12	.150	.159	.178	.178	.215	.226	.232	.225	.212	.220			
25.5	12	-.125	-.125	-.165	-.165	-.178	-.185	-.194	-.200	-.203	-.210			
35.5	12	.057	.040	.040	.038	.039	.045	.054	.060	.064	.074			
(c) Position C														
29	4.05	0.005	0.005	0.000	-0.012	-0.015	-0.049	-0.057	-0.063	-0.065				
39	4.05	-.050	-.035	-.030	-.015	-.018	-.045	-.052	-.055	-.057				
49	4.05	-.014	-.014	-.015	-.015	-.020	-.020	-.020	-.022	-.024	-.025			
22.25	8.0	-.050	-.065	-.072	-.075	-.125	-.135	-.148	-.150	-.152	-.155			
32.25	8.0	-.014	.020	.020	.020	.020	.018	.015	.015	.012	.010			
42.25	8.0	-.010	-.015	-.015	-.015	-.015	-.020	-.020	-.025	-.026	-.030			
15.5	12	-.195	-.236	-.244	-.252	-.267	-.270	-.285	-.292	-.295				
25.5	12	.028	-.035	-.035	-.030	-.018	-.015	-.010	-.008	-.005	.013			
35.5	12	.016	.016	.016	.012	.015	.014	.012	.012	.017	.020			

TABLE 13.- VERTICAL-STRUT PRESSURES FOR SUPERSONIC NOZZLE ($M = 3.04$)

Orifice ordinates	x/D_T	z/D_T	Incremental strut pressure coefficients for $P_{t,c}/P_\infty$ of -										
			10	20	30	40	50	60	70	80	90	100	110
(a) Position A													
29	4.05	-0.010	-0.035	-0.070	-0.120	-0.157	-0.175	-0.187	-0.190	-0.200	-0.213		
39	4.05	-0.000	-0.001	-0.022	-0.044	-0.040	-0.023	-0.045	-0.080	-0.080	-0.065		
49	4.05	-0.007	-0.013	-0.017	-0.020	-0.025	-0.025	-0.025	-0.022	-0.020	-0.020		
22.25	8.0	.100	.100	.127	.170	.205	.205	.181	.173	.176	.190		
32.25	8.0	-.010	-.030	-.060	-.095	-.124	-.139	-.147	-.157	-.162	-.168		
42.25	8.0	-.015	-.029	-.035	-.035	-.035	-.029	-.027	-.035	-.035	-.035		
15.5	12	-.010	-.002	-.002	-.002	-.002	-.002	-.003	-.004	-.005	-.005		
25.5	12	.008	.040	.090	.124	.135	.140	.142	.135	.123	.123		
35.5	12	-.005	-.008	-.014	-.017	-.021	-.022	-.020	-.021	-.021	-.021		
(b) Position C													
29	4.05	0.010	0.000	-0.010	-0.025	-0.038	-0.048	-0.055	-0.059	-0.060	-0.065	-0.067	-0.069
39	4.05	-.025	-.032	-.035	-.037	-.040	-.044	-.048	-.053	-.057	-.062	-.067	-.073
49	4.05	-.008	-.010	-.010	-.012	-.015	-.015	-.015	-.015	-.022	-.024	-.024	-.024
22.25	8.0	-.030	-.050	-.069	-.086	-.100	-.107	-.110	-.115	-.117	-.120	-.125	-.130
32.25	8.0	.020	.025	.028	.032	.035	.035	.035	.030	.030	.022	.018	.015
42.25	8.0	-.017	-.020	-.019	-.016	-.016	-.018	-.020	-.024	-.025	-.029	-.032	-.040
15.5	12	-.127	-.163	-.187	-.205	-.220	-.229	-.237	-.244	-.250	-.256	-.263	-.275
25.5	12	-.010	-.014	-.013	-.016	-.020	-.018	-.011	-.014	-.025	-.024	-.016	-.048
35.5	12	.024	.026	.026	.023	.023	.023	.020	.020	.020	.018	.020	.020

TABLE 14.- VERTICAL-STRUT PRESSURES FOR TWO-DIMENSIONAL SUPERSONIC NOZZLE ($M = 1.71$)

Orifice ordinates		Incremental strut pressure coefficients for $p_{t,c}/p_{\infty}$ of -												
x/D_T	z/D_T	10	20	30	40	50	60	70	80	90	100	110	120	130
(a) Position A														
29	4.05	-0.070	-0.105	-0.140	-0.198	-0.227	-0.240							
39	4.05	-0.078	-0.028	-0.040	-0.052	-0.065	-0.075							
49	4.05	-0.015	-0.017	-0.020	-0.024	-0.025	-0.030							
22.25	8.0	.064	.145	.170	.163	.148	.135							
32.25	8.0	-.008	-.008	-.025	-.065	-.110	-.142							
42.25	8.0	-.015	-.030	-.040	-.045	-.060	-.080							
15.5	12	-.002	-.005	-.005	-.007	-.010	-.010							
25.5	12	.024	.070	.095	.092	.097	.110							
35.5	12	.004	.001	-.009	-.018	-.024	-.025							
(b) Position B														
29	4.05	0.015	0.008	-0.015	-0.052	-0.085	-0.112							
39	4.05	-0.015	-0.027	-0.038	-0.045	-0.055	-0.060							
49	4.05	-.002	-.004	-.005	-.008	-.010	-.011							
22.25	8.0	-.080	-.125	-.172	-.211	-.235	-.262							
32.25	8.0	.025	.035	.028	.035	.035	.032							
42.25	8.0	-.005	-.010	-.017	-.020	-.025	-.032							
15.5	12	.050	.125	.155	.160	.170	.158							
25.5	12	-.040	-.050	-.076	-.105	-.115	-.118							
35.5	12	-.005	.003	.015	.020	.018	.017							



L-57-836.1
Figure 1.- Typical test setup.

L-1614

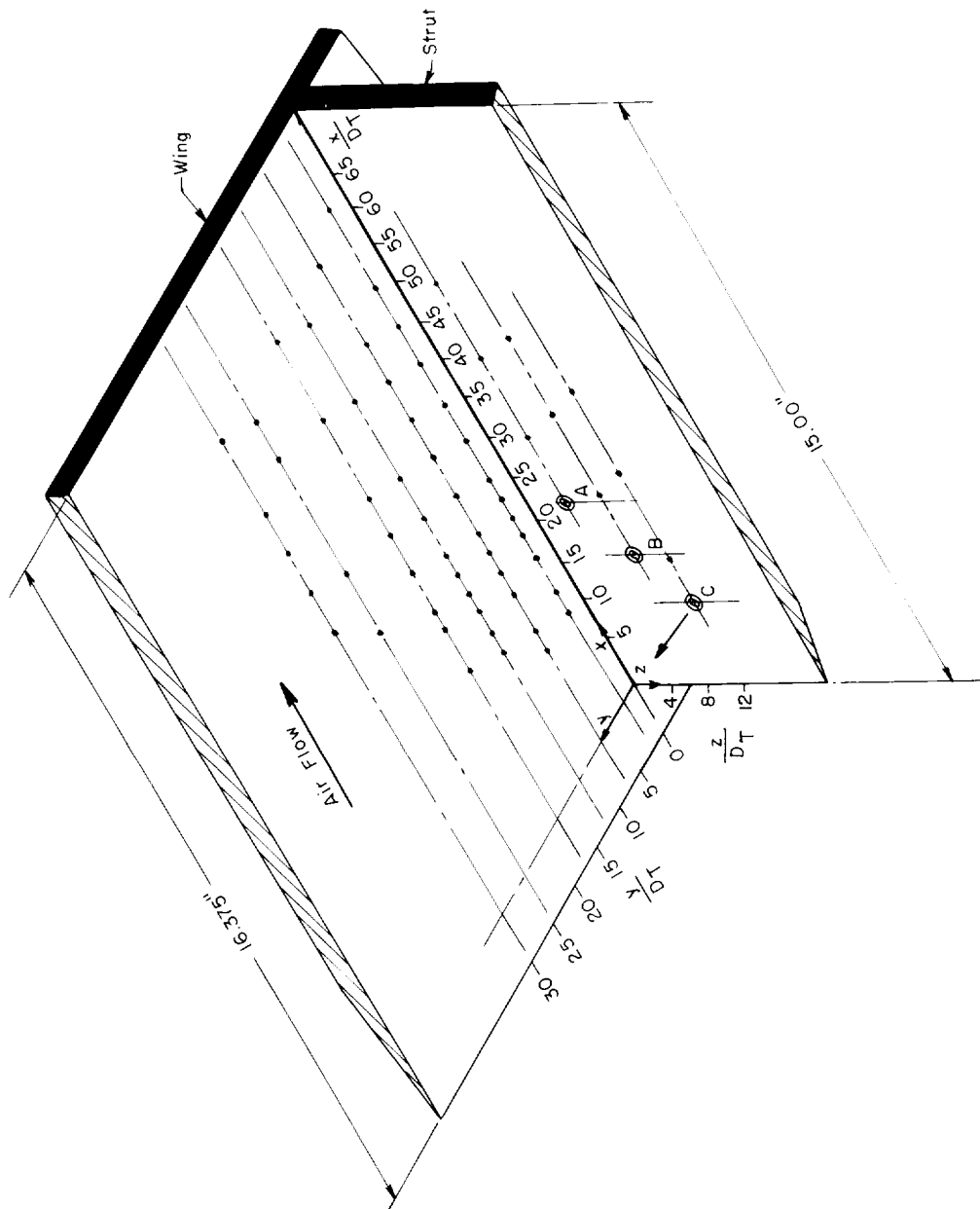


Figure 2.- Three-dimensional drawing of arrangement of flat-plate wing and vertical strut with wing and strut static-pressure orifices and rocket-nozzle position indicated.

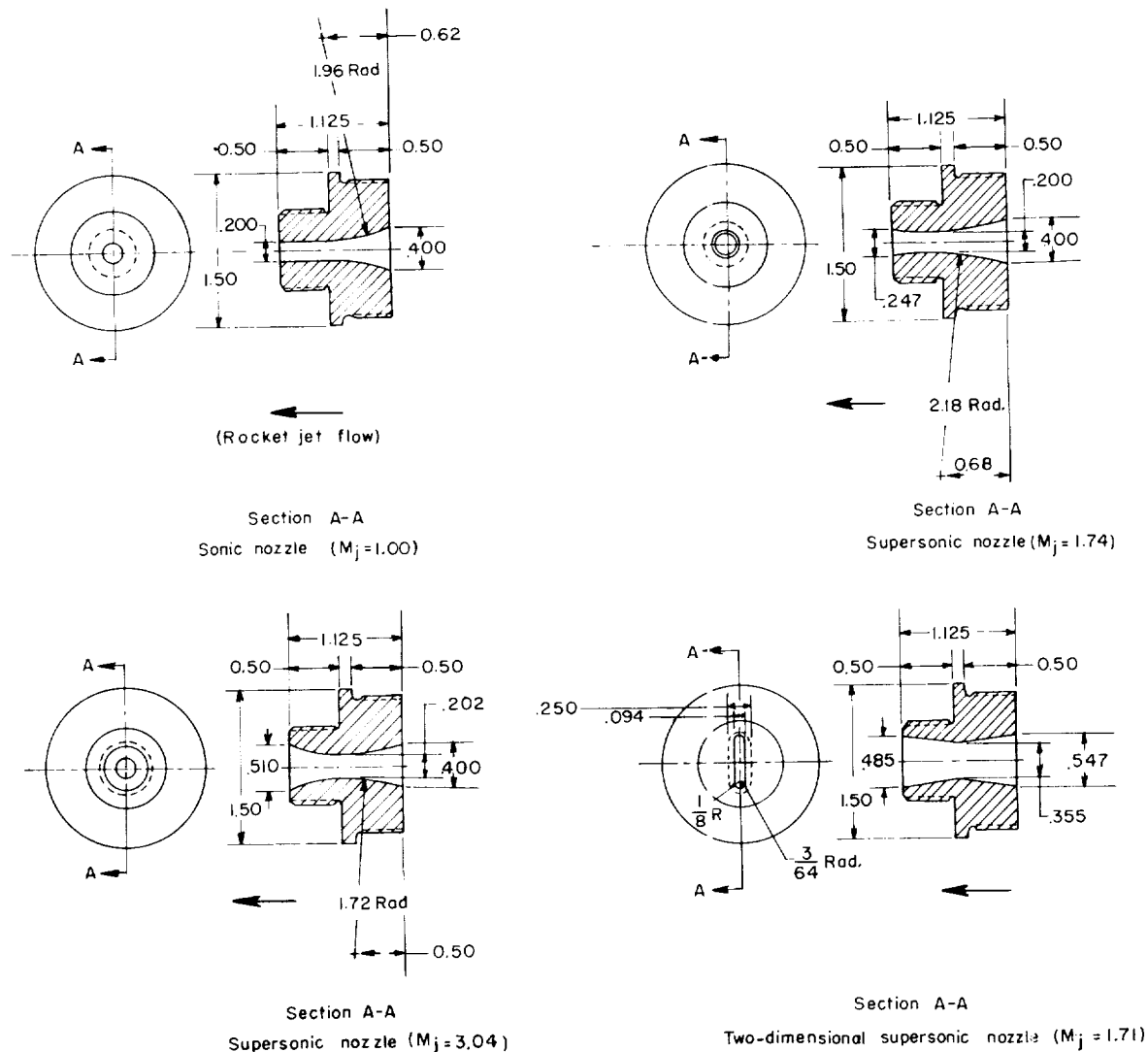


Figure 3.- Nozzle geometries and parameters used in the investigation.
 $\gamma = 1.25$ for rocket gases. (All dimensions are in inches.)

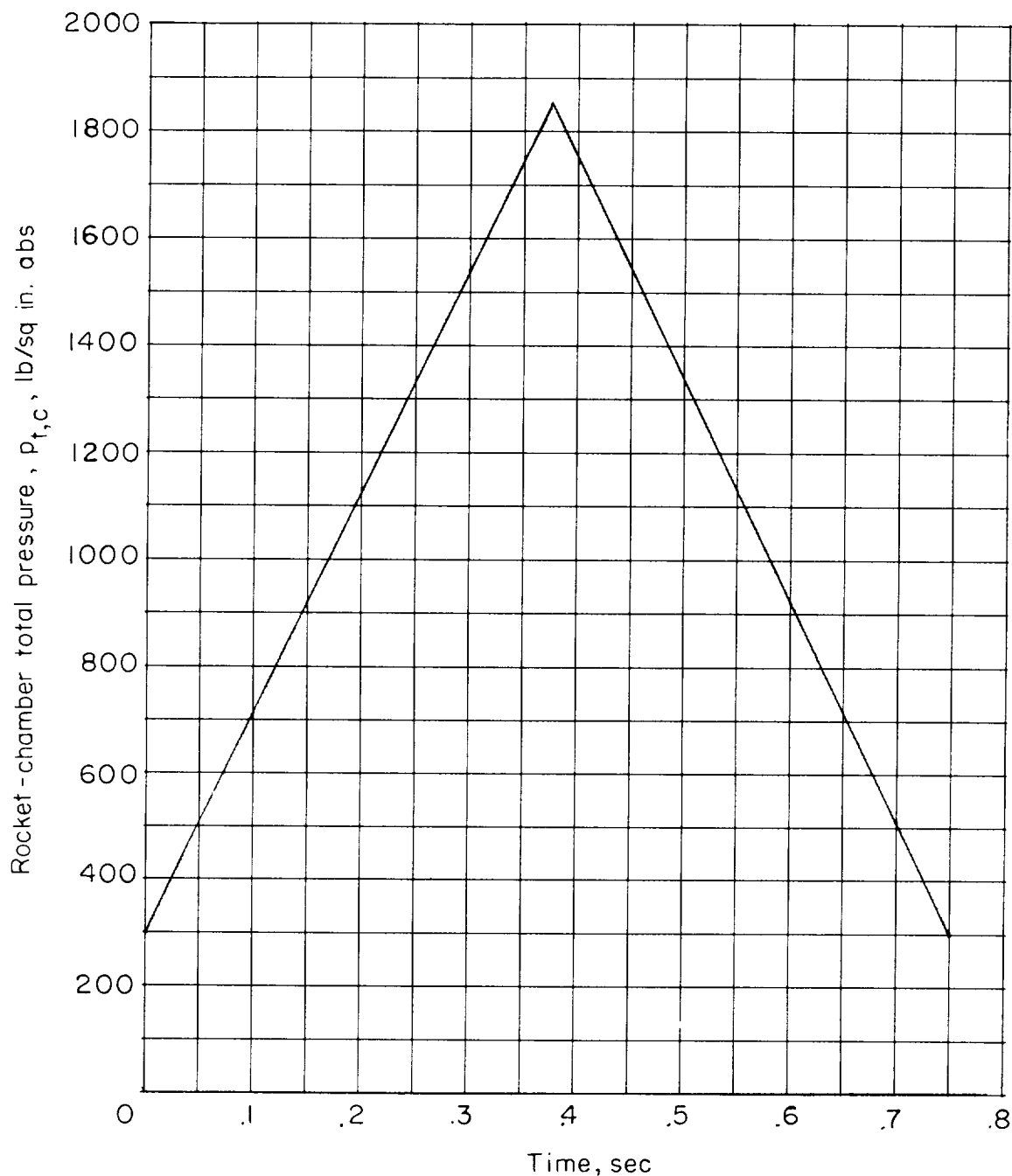
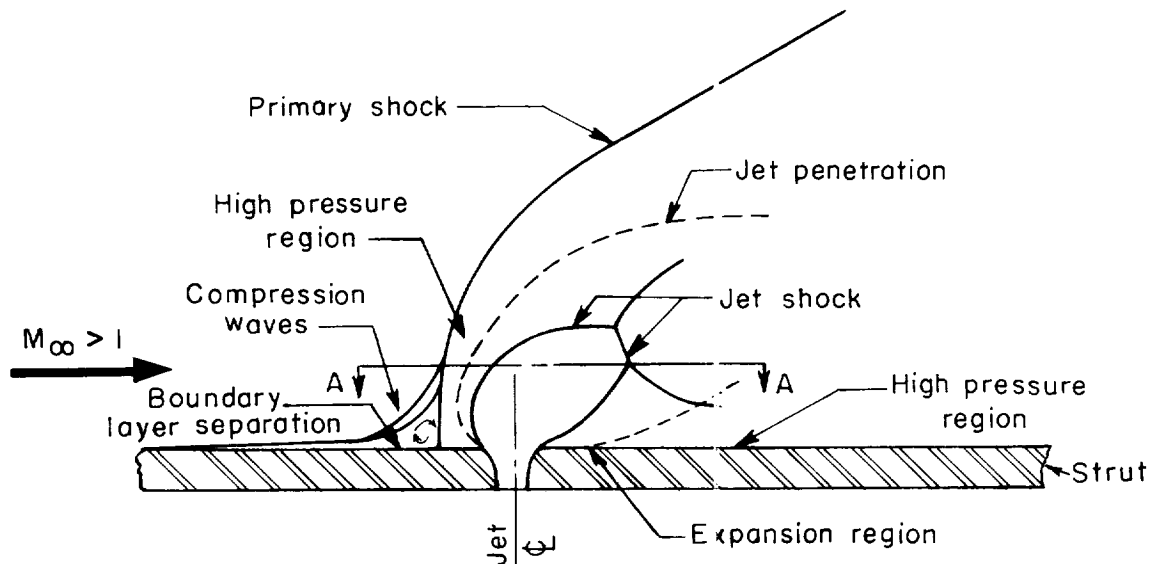
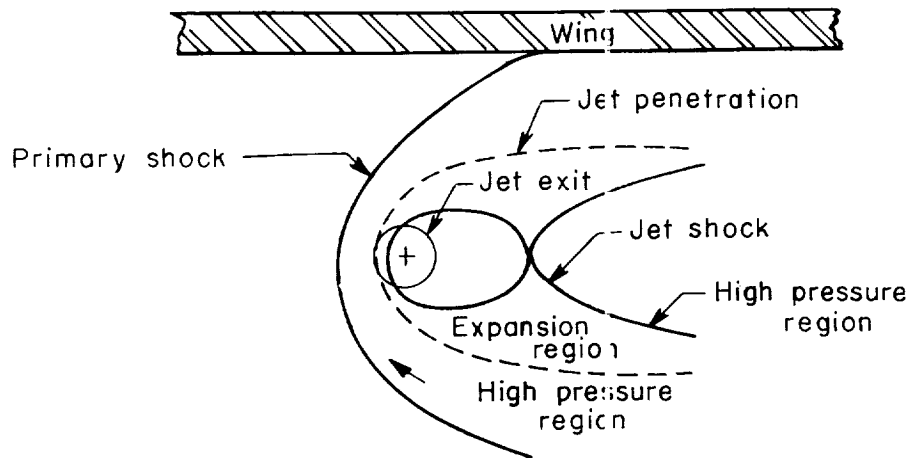


Figure 4.- Rocket-chamber-pressure design curve.



(a) Flow field and nomenclature.



(b) Section A-A of flow field.

Figure 5.- Drawing and nomenclature of the flow field about a jet exhausting normal to free stream.

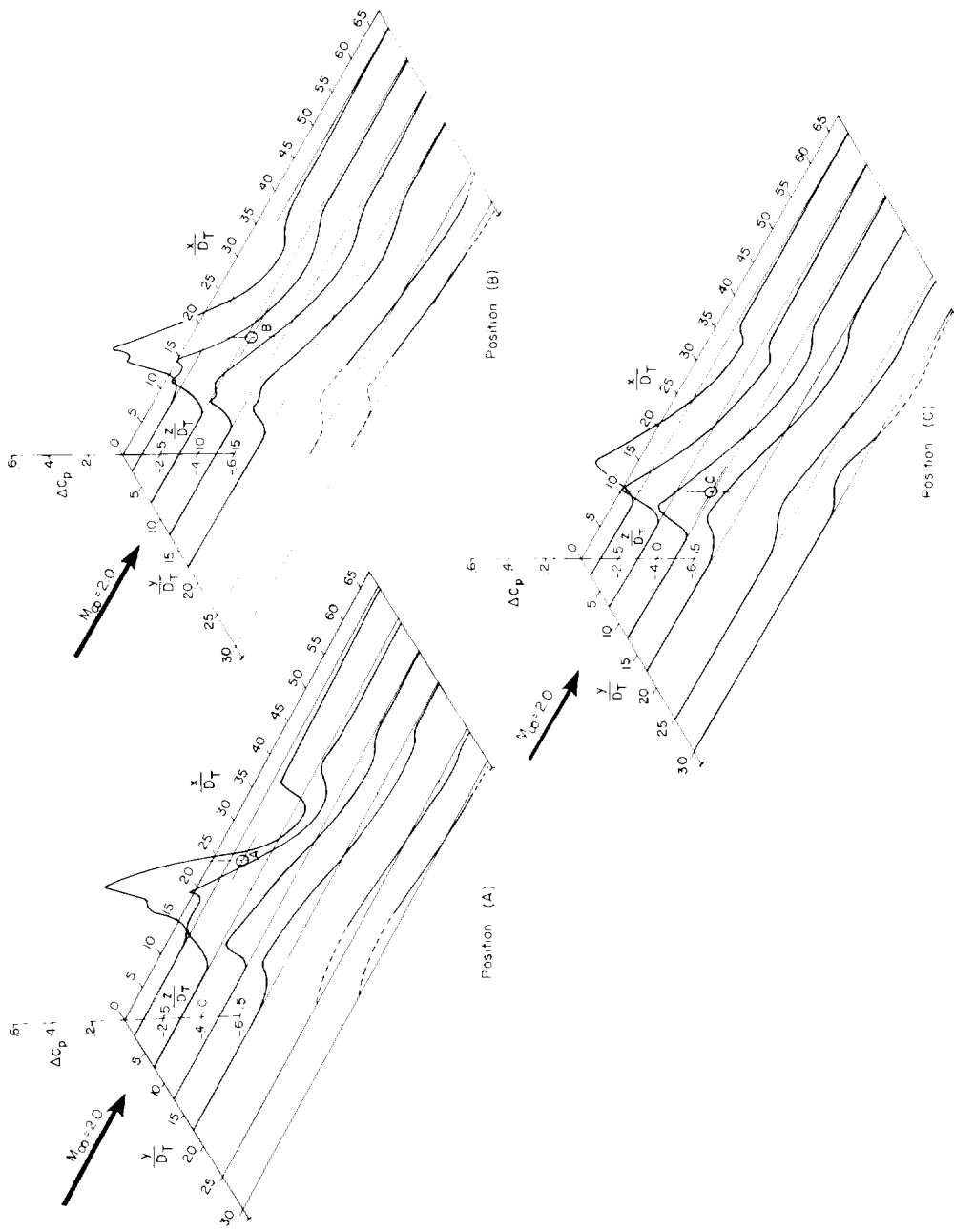


Figure 6.- Variation of chordwise and spanwise incremental pressure coefficient with nozzle position for sonic jet ($M_j = 1.0$) and pressure ratio of 58. Dashed portions of curves indicate omission of pressure measurements.

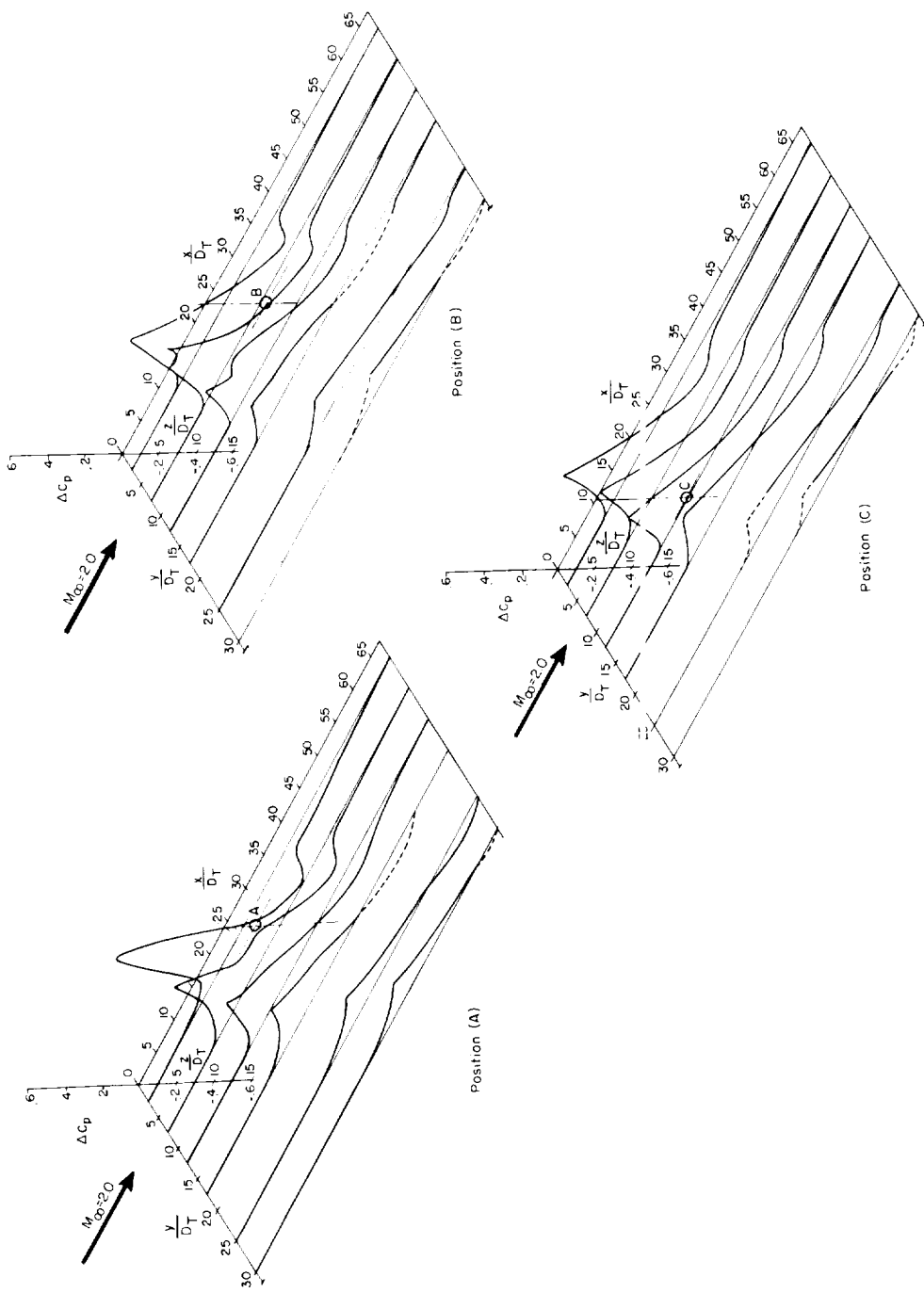


Figure 7.- Variation of chordwise and spanwise incremental pressure coefficient with nozzle position for supersonic jet ($M_j = 1.74$) and pressure ratio of 58. Dashed portions of curves indicate omission of pressure measurements.

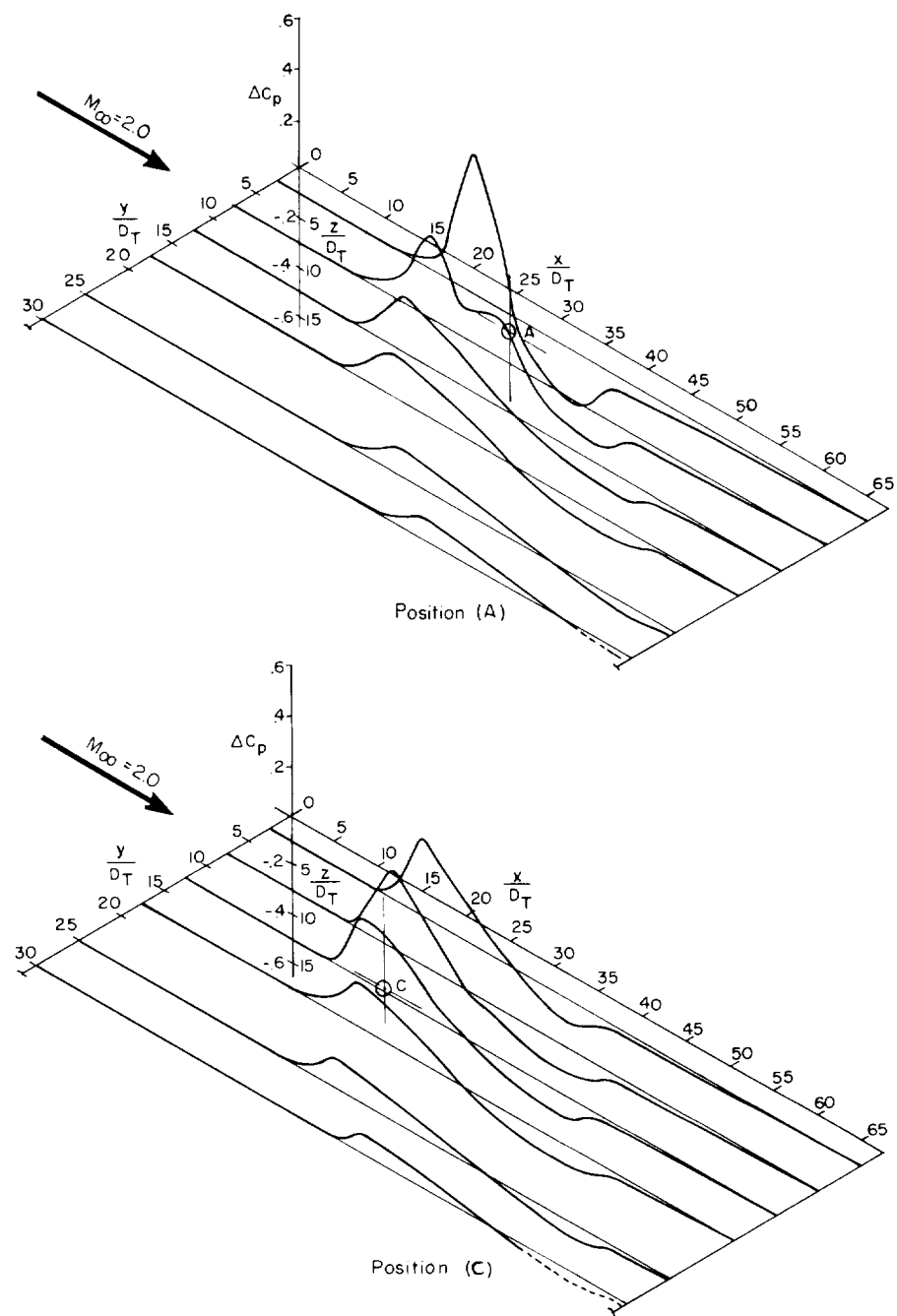


Figure 8.- Variation of chordwise and spanwise incremental pressure coefficient with nozzle position for supersonic jet ($M_j = 3.04$) and pressure ratio of 58. Dashed portions of curves indicate omission of pressure measurements.

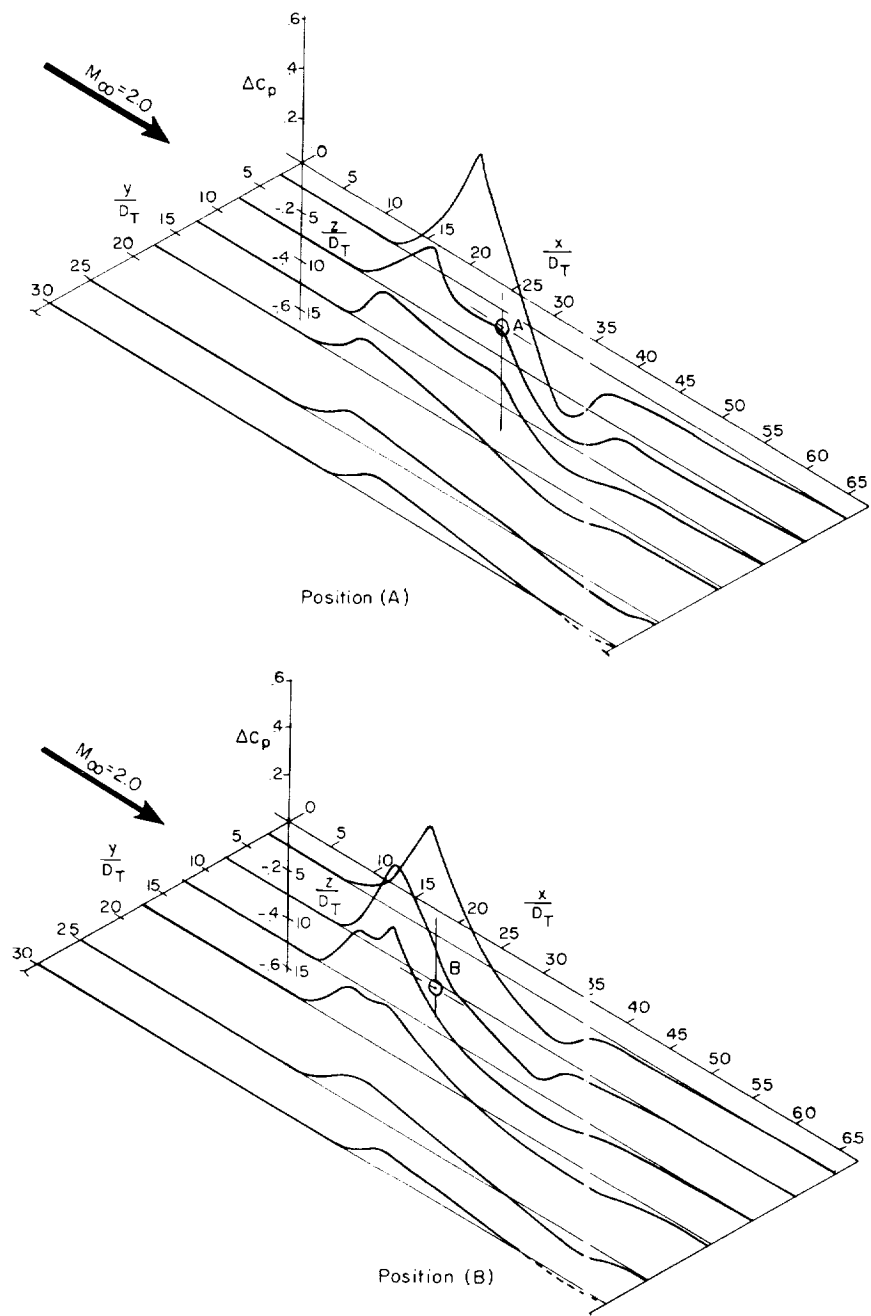


Figure 9.- Variation of chordwise and spanwise incremental pressure coefficient with nozzle position for two-dimensional supersonic jet ($M_j = 1.71$) and pressure ratio of 58. Dashed portions of curves indicate omission of pressure measurements.

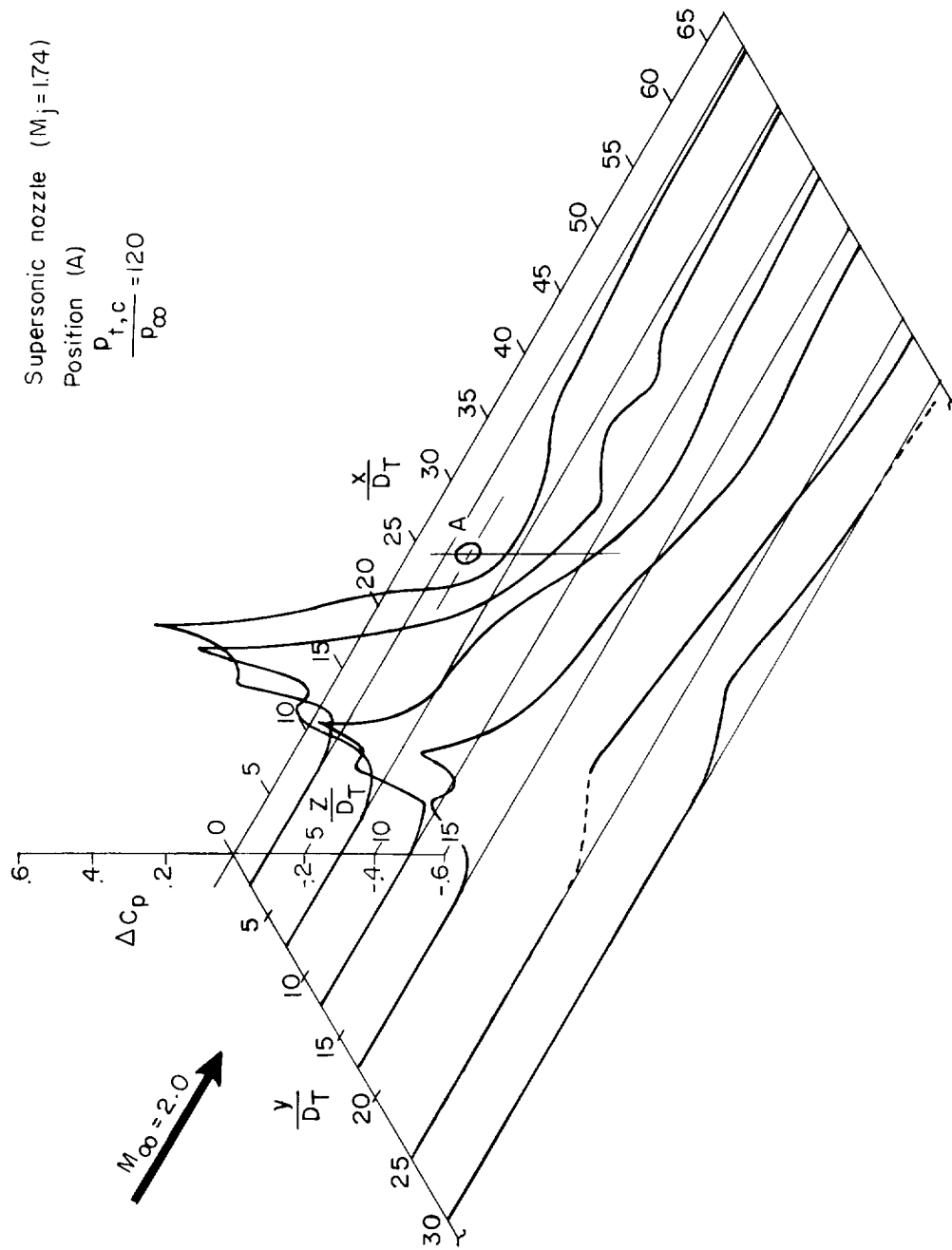


Figure 10.- Chordwise and spanwise incremental pressure coefficient for supersonic nozzle ($M_j = 1.74$) in position A and for pressure ratio of 120. Dashed portions of curves indicate omission of pressure measurements.

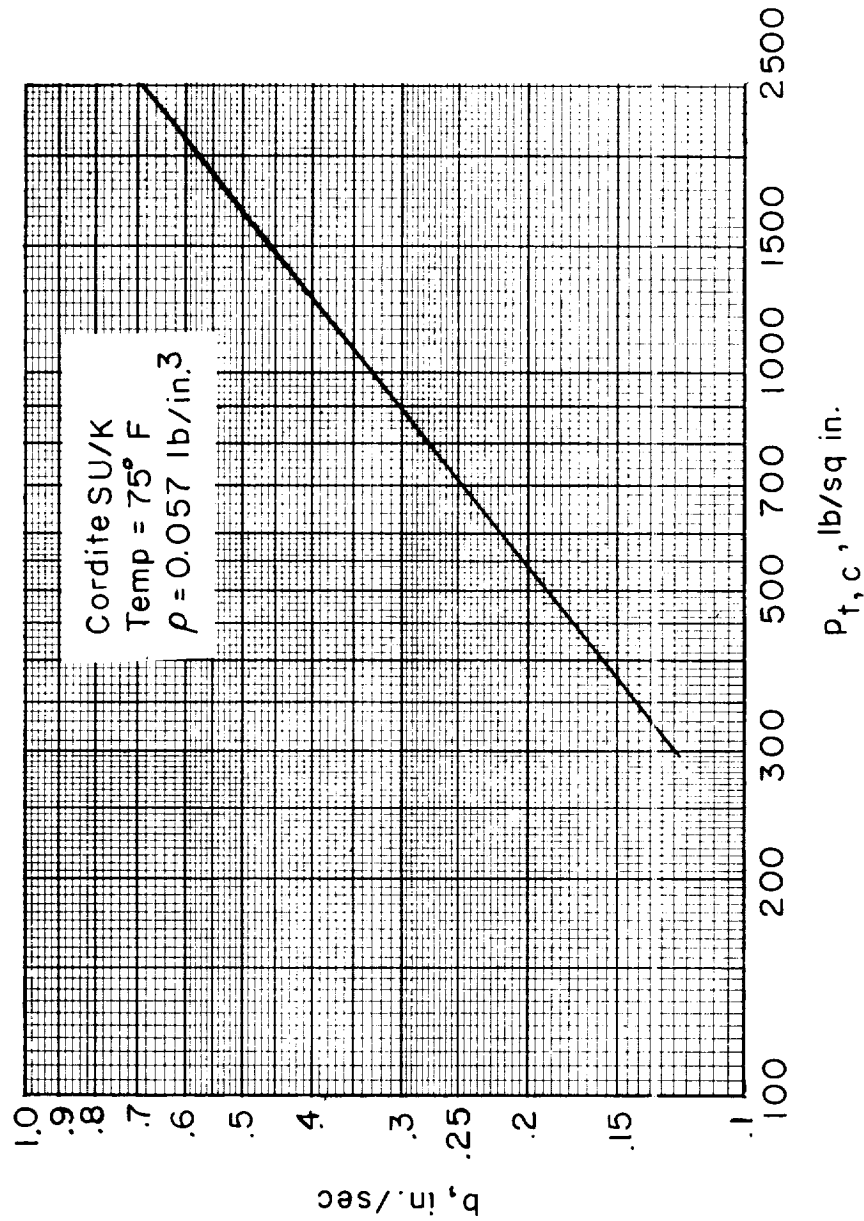


Figure 13.- Burning rate as a function of combustion-chamber pressure.

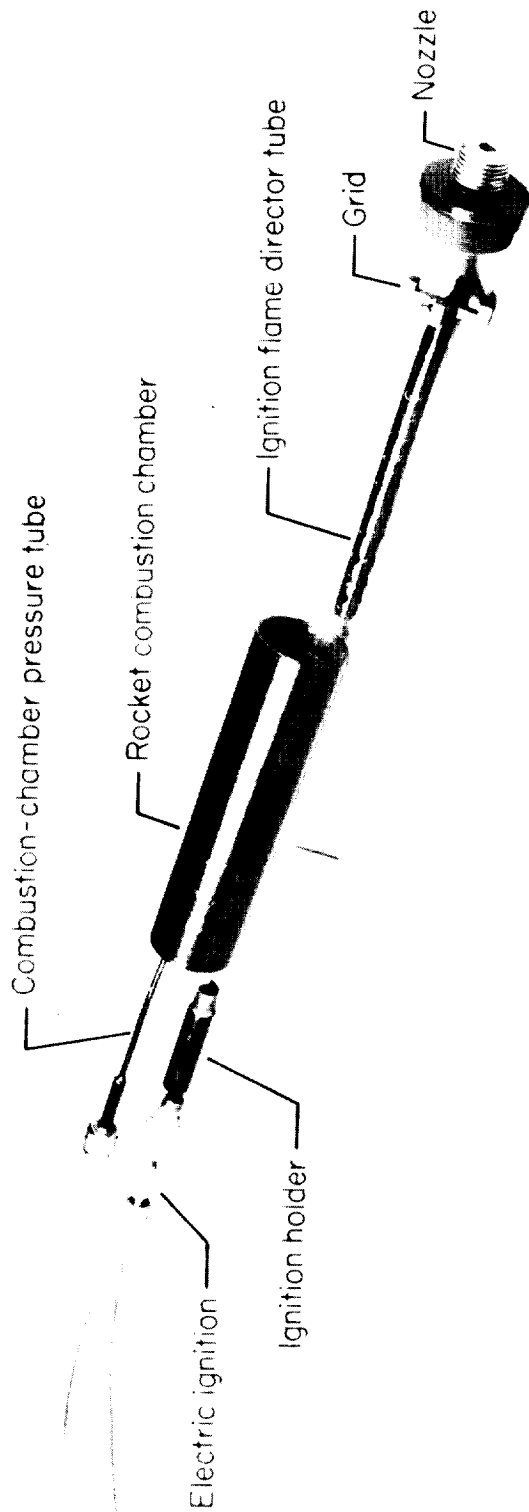


Figure 14.- Rocket components used in the investigation. L-57-3208.1

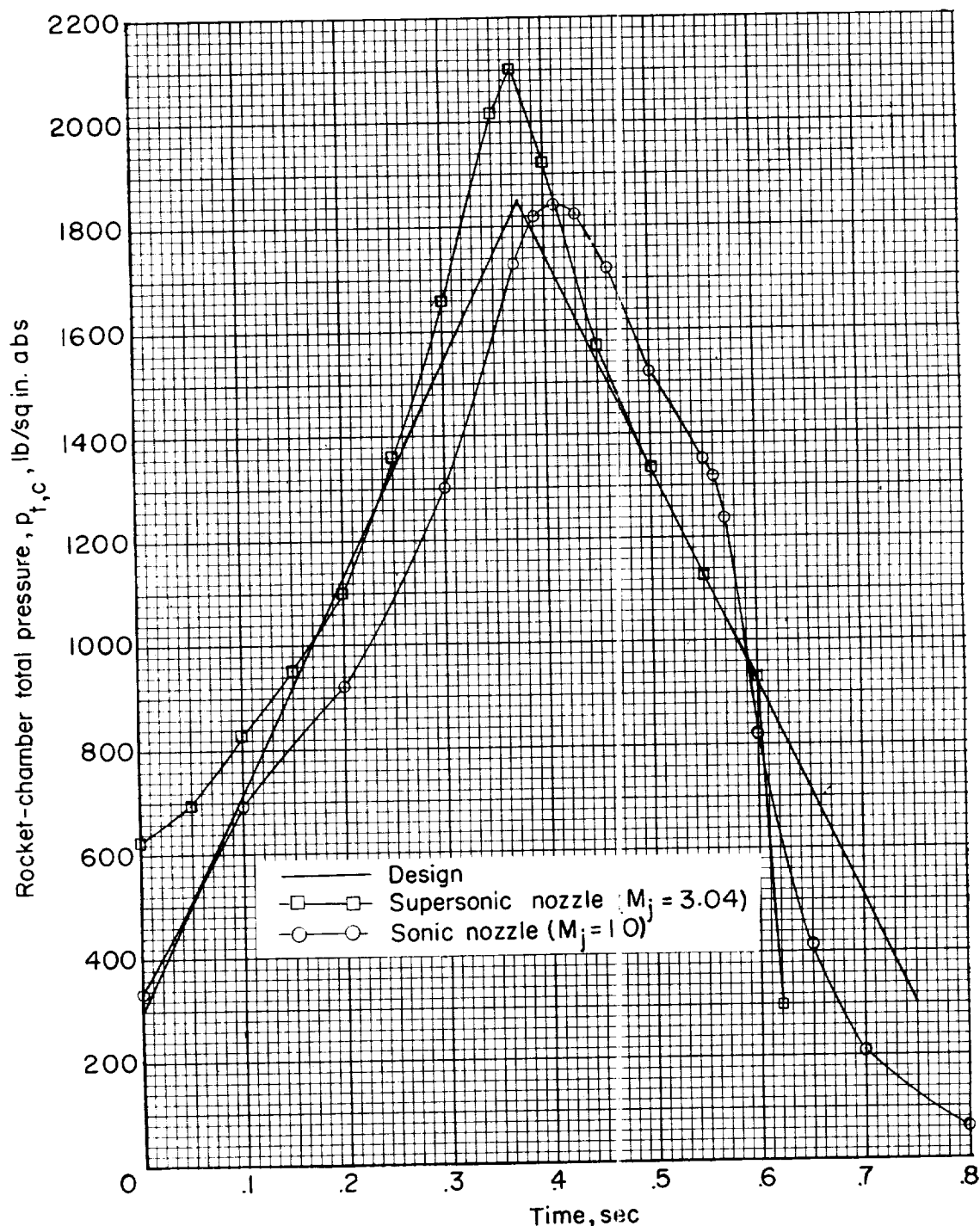


Figure 15.- Comparison between design and test values of time histories of rocket-chamber total pressure.

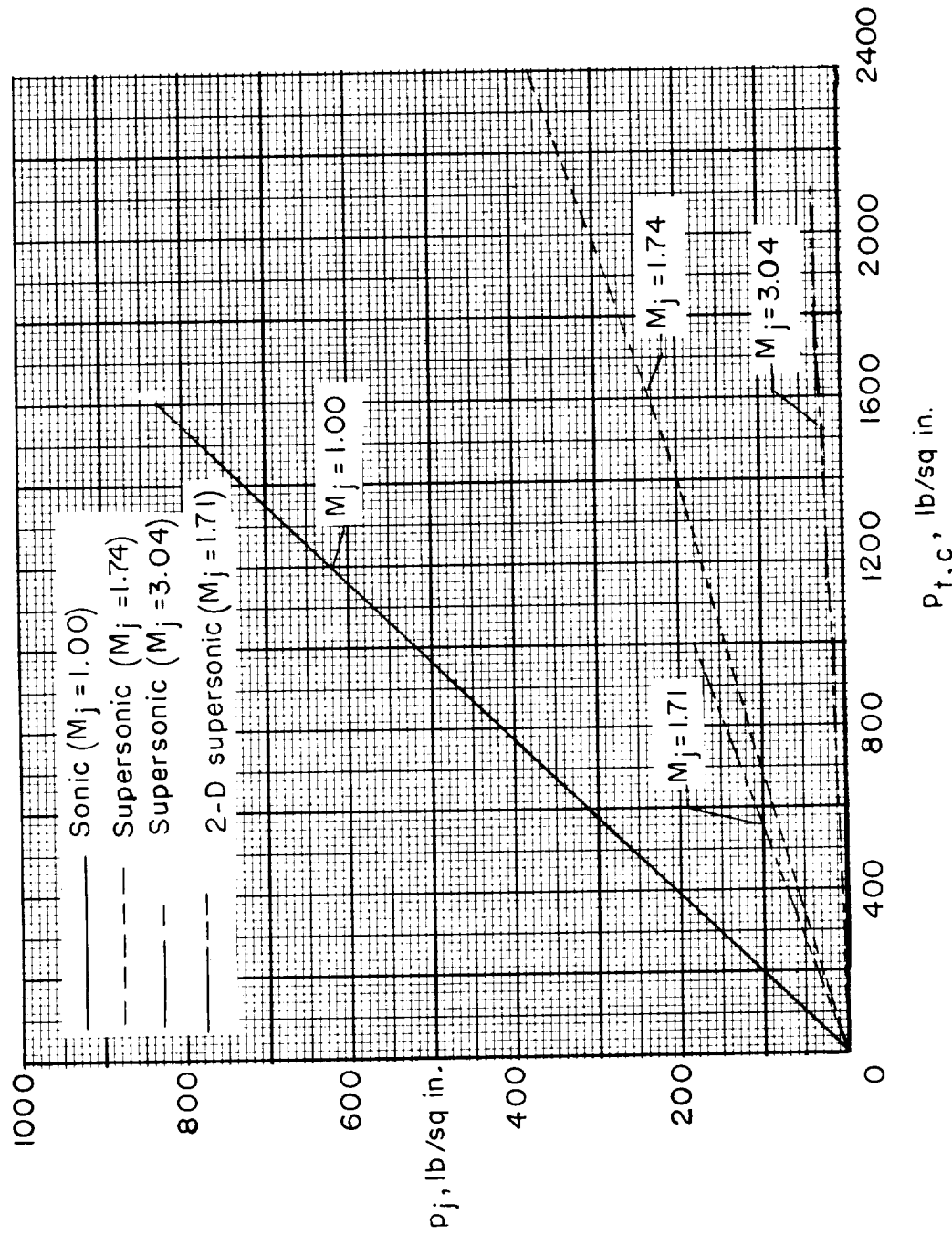


Figure 16.- Calibration curves of jet-exit static pressure as a function of rocket-chamber total pressure for the nozzle types used.

